A comprehensive study of effective parameters on the thermal performance of porous media micro combustor in thermo photovoltaic systems

Bajelani, Mehran; Ansari, Mohammad Reza; Nadimi, Ebrahim

DOI:
10.1016/j.applthermaleng.2023.120846

Document Version
Publisher's PDF, also known as Version of record

Citation for published version (Harvard):
Bajelani, M, Ansari, MR & Nadimi, E 2023, 'A comprehensive study of effective parameters on the thermal performance of porous media micro combustor in thermo photovoltaic systems', *Applied Thermal Engineering*, vol. 231, 120846. https://doi.org/10.1016/j.applthermaleng.2023.120846

Applied Thermal Engineering 231 (2023) 120846

Contents lists available at ScienceDirect

Applied Thermal Engineering

journal homepage: www.elsevier.com/locate/apthermeng

Research Paper

A comprehensive study of effective parameters on the thermal performance of porous media micro combustor in thermo photovoltaic systems

Mehran Bajelani [a], Mohammad Reza Ansari [a], Ebrahim Nadimi [b,*]

[a] Department of Mechanical Engineering, Tarbiat Modares University, Tehran, Iran
[b] Department of Thermal Technology, Faculty of Energy and Environmental Engineering, Silesian University of Technology, Gliwice, Poland

ARTICLE INFO

Keywords:
Thermo-photovoltaic (TPV) system
Micro-combustor
Porous medium
CFD

ABSTRACT

Low thermal performance is one of the biggest challenges of using micro combustor in Thermo-photovoltaic (TPV) system. In this study, a novel micro-combustor with porous media was designed and installed to enhance energy and exergy performance. Furthermore, the effects of several effective parameters including different porous media materials, length, porosity coefficient, and inlet mass flow on energy efficiency, exergy, entropy generation, wall temperature and its uniformity were studied. A comprehensive CFD model for using porous media in the micro-combustor of TPV systems was proposed. Results showed utilizing porous media significantly improve the exergy efficiency and energy output of TPV system. Therefore, using a 6 mm long porous media increased the average wall temperature by 111 K compared to the case without porous media. Additionally, the uniformity coefficient of the wall temperature decreased by 80.05 %, from 4.58 % to 0.89 %. This reduction increased the temperature uniformity of the outer wall of the micro-combustor with porous media compared to the case without a media, increasing the system's lifetime. Moreover, the 6 mm-long porous media enhanced radiation efficiency and exergy efficiency by 37 % and 79.7 %, respectively, compared to the conventional micro combustor. The total energy conversion efficiency from the fuel chemical energy to electric power increased from 8.9 % to 12.32 %.

1. Introduction

Due to environmental issues of using fossil fuels, industries are turning to new renewable energy sources that do not have the problems of the current fossil fuels. Industrial owners have recently shown interest in electricity generation from systems with non-fossil sources. Using the TPV system is one of the viable methods to generate electricity, which performs based on the direct conversion of fuel chemical energy to electrical energy [1]. However, proper power generation is the most crucial challenge in using this system, and reducing the prime cost of cells is highly significant in increasing its commercialization potential [2].

The demands of various industries in the world for portable energy sources at a small scale are high. Hence, micro-power generators (MPG) have been developed to convert different forms of energy to electricity [3]. Therefore, it is necessary to establish a cost-efficient system based on existing equipment for the utilization of TPV [4]. Fig. 1 illustrates the conceptual structure of a TPV cell for electricity generation, whose components are comprised of the following [5]:

- Combustor
- Optical filter
- Photovoltaic (PV) cell

Given the direct relationship between the outer surface of the combustor and the electric power generation, a higher surface-to-volume ratio of the combustor results in increased thermal efficiency of the system [6]. Therefore, the combustor is used at the micro scale to increase the volume to area ratio of micro-combustor at the microscale. Low thermal efficiency is one of the most significant defects of micro-TPV generators [7]. Considering that the micro-combustor in these generators has the greatest influence on determining the overall efficiency of power generators [8], researchers have studied the performance of micro-combustors to enhance their efficiency.

Using mixed fuels in the micro-combustor is one of the practical methods in enhancing the performance of micro-TPV systems. In this regard, fuels such as H_2 [9–13], propane [14–17], and methane [18,19] are commonly used in these systems., Tang et al. [20] compared these three hydrocarbon fuels in the micro-combustor at different equivalence ratios, it was proven that the hydrogen/air mixture has a wider and

* Corresponding author.
E-mail address: enadimi@polsl.pl (E. Nadimi).

https://doi.org/10.1016/j.applthermaleng.2023.120846
Received 14 February 2023; Received in revised form 2 May 2023; Accepted 20 May 2023
Available online 7 June 2023

Nomenclature

$A_i\,(m^2)$	The surface area of grid cell i on the wall
$T_i\,(K)$	The temperature of grid cell i
$E_T\left(\frac{J}{kg}\right)$	total fluid energy
I	Unit tensor
d(m)	particle diameter
$h\left(\frac{W}{m^2.K}\right)$	Heat transfer coefficient
$h_j\left(\frac{J}{kg}\right)$	Enthalpy of species j
$K_s\left(\frac{W}{m.K}\right)$	Solid material thermal conductivity
$K_{eff}\left(\frac{W}{m.K}\right)$	Effective conductivity
$S_f\left(\frac{W}{m^3}\right)$	Fluid enthalpy source term
p(Pa)	Pressure
P_0(Pa)	Atmosphere pressure 101,325
$R_{outlet}\left(\frac{J}{kg.K}\right)$	Specific gas constant at the outlet
$R_u\left(\frac{J}{mol.K}\right)$	Universal gas constant
$\overline{W}$	Mean molecular weight of the mixture
$\vec{J}_j\left(\frac{kg}{m^2.s}\right)$	Diffusion flux of species j
L(mm)	The length of the micro-combustor
D(m)	The diameter of the micro-combustor
T(K)	Temperature
T_{ave}(K)	Mean temperature
T_m(K)	Mean outer wall temperature
T_{sur}(K)	Surrounding temperature
$\dot{E}x_{loss}$	The exergy loss
$\dot{E}_{loss}$(W)	Energy brought away by the exhaust gases
$\dot{m}\left(\frac{kg}{s}\right)$	Total mass flow rate
$\dot{m}_{H2}\left(\frac{kg}{s}\right)$	The mass flow rate of hydrogen at the inlet
$u\left(\frac{J}{kg}\right)$	Specific internal energy
n_j	The number density of species j
Yj	Mass fraction of species j
$\vec{u}$	Velocity vector
$\dot{S}_{gen}$	The entropy generation rate
$C_{P_{outlet}}\left(\frac{J}{kg.K}\right)$	Specific heat capacity at the outlet

Greek symbols

$\dot{S}_{gen}$	The entropy generation rate
e	Surface emissivity
η_{Rad}	Combustor radiative efficiency
η_{TPV}	Thermo photovoltaic system efficiency
η_{Tot}	Total efficiency
$\rho\left(\frac{kg}{m^3}\right)$	Density
$\sigma\left(\frac{W.m}{k^4}\right)$	Stefan-Boltzmann constant
ω_j	The rate of reaction of the jth species
μ(Pa.s)	Molecular viscosity
$\mu_j\left(\frac{J}{kg}\right)$	The chemical potential of species j

Abbreviations

TPV	Thermophotovoltaic
rad	Radiation
con	Conversion
LHV	Low heat value
sur	Surrounding
eff	Effective conductivity
in	Inlet
MPG	Micro-power generators
CFD	Computational fluid dynamics

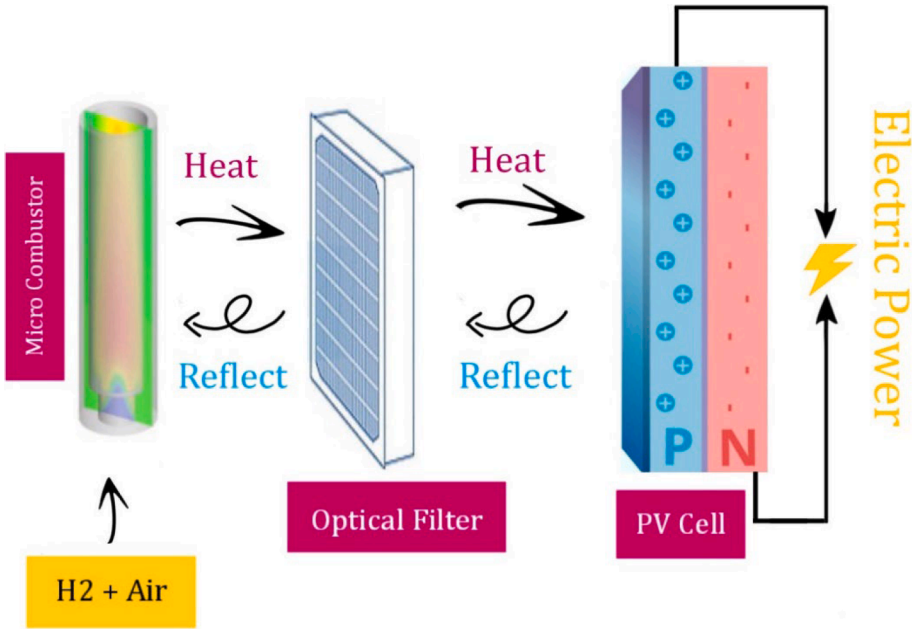

Fig. 1. An illustration of the conceptual model of a TPV cell.

more stable flammability limit compared to the other two fuels. Under similar input energy ratios, maximum wall temperature and temperature gradient for the hydrogen/air mixture were reported higher than the methane/air and propane/air mixtures. Also, methane showed the most uniform temperature distribution in the outer wall of the combustor and the highest average wall temperature among the three

Table 1
A summary of the studies conducted on combustors of TPV systems with porous media.

Reference	Combustor		Fuel	Research method		Porous	Studied parameter
	Planner	Cylindrical		Exp.	Num.		
Chou et al. [33]	–	✓	H_2	–	✓	SiC	• Porosity
Pan et al. [34]	–	✓	H_2	–	✓	SiC Si_3N_4 Al_2O_3	• Material of porous media H_2/O_2 equivalence ratio Porosity Mixture flow rate
Mustafa et al. [35]	✓	–	kerosene–VCO	✓	–	Porous alumina	• Fuel–air equivalence ratios
Bani et al. [36]	–	✓	H_2	✓	✓	SiC	• Variation of the distance between the TPV cell and the external surface of the combustor
Qian et al. [11]	✓	–	H_2	–	✓	–	• H_2 equivalence ratio inlet velocities
Peng et al. [15]	–	✓	$C_3H_8H_2$	✓	✓	Ten kinds of porous media	• Various PPI Porosity Mixture flow rate Fuel–air equivalence ratios Varied wire diameter of porous medium
Peng et al. [31]	–	✓	H_2	✓	✓	–	• Multi-PM-layers Porosity H_2 equivalence ratio Mixture flow rates.
Wang et al. [37]	✓	–	C_3H_8	✓	✓	Nickel foam	• C_3H_8 equivalence ratio Inlet velocities
Gentillon et al. [38]	–	✓	CH_4	✓	–	–	• Three different designs of porous media Different PV cells
Bubnovich et al. [39]	–	✓	CH_4	✓	–	Al_2O_3	• CH_4 equivalence ratio Volumetric flow rate
Yang et al. [40]	–	✓	H_2	✓	–	SiC	• Mixture flow rate H_2 equivalence ratio
Jun Li et al. [41]	✓	–	H_2	–	✓	SiC	• Mixture flow rate H_2 equivalence ratio Porosity Thermal conductivity
Peng et al. [32]	–	✓	H_2	✓	✓	SS304	• H_2 equivalence ratio Various of Combustor length Various of Combustor diameter
Peng et al. [42]	–	✓	H_2	–	✓	–	• Various of outer wall thickness Various of flame location H_2 equivalence ratio
Present research	–	✓	H_2	–	✓	SiC Si_3N_4 Al_2O_3 SS304	• Material of porous media Inlet velocities Various Porous Medium Length Thermal conductivity Porosity

fuels. Also, L. Han et al. [21] used the H_2/NH_3 fuel mixture for the TPV system to enhance the thermal performance and to stabilize the flame in the micro-combustor. They designed a wavy geometry for the micro-combustor and revealed that it is possible to obtain a much higher average wall temperature and a more stable flame than typical combustors by utilizing the H_2/NH_3 fuel mixture in such wavy micro-combustors. Furthermore, the effects of the H_2/NH_3 mixture on the NOx emission were fully analyzed, and a 21.2 % reduction in NOx emission in the wavy micro-combustor was reported.

Peng et al. [14] conducted a numerical analysis of the premixed H_2/air combustion with different ratios of the propane mixture C_3H_8 in the micro-combustor to improve energy efficiency and the system's output power. The results revealed that adding 5 % of C_3H_8 to the premixed mixture would enhance the flame regime and its stability, cause the uniform distribution of the outer wall temperature, and reduce heat loss.

The effect of modifying in the geometry of the micro-combustor on increasing the surface subjected to heat transfer has also been investigated in recent years. This is because employing efficient configurations improve heat transfer from hot gases into the combustor walls, which reduces the temperature of output gases and prevents energy losses in the micro-combustor [22]. Akhtar et al. [23] investigated the effect of circular, rectangular, triangular, and trapezoidal cross-sections on micro-combustors. Hence, they concluded that the rectangular and trapezoidal cross-sections had the highest efficiency in energy conversion. In their other study, Akhtar et al. [24] analyzed the impact of curved channels on heat transfer, flame stability, and emission levels in a circular micro-combustor. Using curved channels increased the outer wall temperature and overall efficiency in energy conversion to 110 K and 7.84 %, respectively, compared to direct channels. However, the flame structure in curved channels showed more instability. Researchers have always attempted to make the wall temperature more uniform and increase radiation efficiency through an optimal design of the micro-combustor geometry. Mansouri [25] designed a new geometry with wavy walls in which using this type of wall would increase the surface-to-volume ratio in the micro-combustor, resulting in enhanced heat transfer. Additionally, an increase in the number of waves in the wall would help the flame move toward the outlet of the micro-combustor. Furthermore, creating cavities in combustor walls is another solution to increase the surface of heat transfer in the micro-combustor. Yang et al. [26] examined the thermal performance of a combustor by creating two cavities in it. According to the results, the new combustor showed a higher and more uniform temperature distribution along the wall. An increase in the number of cavities increased radiation efficiency from 1.25 % in a single-cavity combustor to 1.53 % in a two-cavity

combustor.

With the use of a insert body, such as a fin, conductive sheet, bluff body, or porous medium, some researchers have enhanced energy conversion and flame stability at the microscale. Ziqiang He [27] designed an internal spiral fins in order to reduce heat loss and increase heat transfer. Further, the effect of the geometrical parameters, including internal spiral fin number, length and pitch distance on the thermal performance and exergy efficiency was examined. According to the results, the micro-combustor with 8 spiral fins exhibits the highest exergy efficiency of 66.9 %, which is 6.9 % higher than that of the conventional one at the inlet velocity of 5 m/s. furthermore results revealed that the micro-combustor with 8 spiral fins obtains the highest energy output is 5.01 W at inlet velocity of 8 m/s. Yang et al. [28] proposed a swirling geometry to enhance the flame stability at the inlet of the micro-combustor. They examined the flame stability mechanism and combustion characteristics at various velocities and equivalence ratios. Their results showed this swirling area causes the heat circulating from solid walls to couple with the swirling flow in recirculating areas, increasing the flame stability. Wu et al. [29] installed a new conductive sheet in a cylindrical micro-combustor to enhance the outer wall temperature and exergy efficiency. The effect of different factors, including the number of sheets, the sheet width, the thickness, and the convergence and divergence angles of the sheet, on the thermal performance of the micro-combustor was examined. According to the results, the proposed conductivity sheet improved the thermal performance of the micro-combustor and the outer wall temperature and the exergy efficiency increased by 108 K and 12.86 %, respectively.

Flame stability is a another crucial parameter in the micro-combustor in improving the performance of the TPV system. Qian et al. [11] placed a bluff body in the micro-combustor for better flame stability and examined its impact on the average wall temperature and system efficiency. According to the results, system efficiency increased by 14.72 % by deploying a buff body compared to the simple system. To improve the heat transfer rate in the micro-combustor, Mohseni et al. [30] analyzed various approaches including using a porous medium, multi-hole blades and setting 24 and 8 tubes in the micro-combustor. Based on the calculations, the micro-combustor with a porous medium performed best, among other designs, in terms of energy through reduction of the exhaust gas temperature by 289 K and the average wall temperature increased by 115 K. Additionally, the temperature distribution on the wall surface became 50.4 % more uniform.

Therefore, using a porous media in the micro-combustor has been one of the latest topics regarding TPV systems in which researchers have shown interest. This is because utilizing a porous media prevents the energy loss and convection heat from the outlet of the micro-combustor, which increases wall temperature, and consequently, reduces heat losses. This increased wall temperature could result in an improvement in radiation efficiency and exergy efficiency, as well as reduce entropy generation in the micro-combustor. A low porosity coefficient could improve flame stability and heat transfer while preventing emissions in the system. Therefore, Peng et al. [31] suggested using a layered porous media with different porosity coefficients per layer to create a balance in the system and proportion between the flame stability and its power. According to their simulation, the combustor with a three-layer porous media with porosity coefficients $p = 0.95 + 0.9 + 0.85$, cause the output electric power and the system efficiency to be high, making it a favorable option as a micro-power generator. Peng et al. [32] examined the premixed H_2/air combustion with and without a porous medium. According to the results, flame stabilization in a micro-combustor with a porous media drastically increased compared to the simple one.

Above literature review shows a micro-combustor with a porous media can improve thermal performance. Table 1 illustrates a summary of all studies conducted using porous media in the micro-combustor of TPV systems. This table shows utilized porous media, different fuel, and the main studied parameter. It is concluded that researcher have carried out studies on improving the flame stability and energy conversion efficiency of micro-combustors. In addition, the effects of porous media on the exergy and combustion of micro-combustor for TPV system are not studied in previous work. However, various porous characteristics in micro-combustor resulting in difference heat transfer mechanisms and thermal performance of micro-combustor. Therefore, in mentioned studies, only one parameter of porous media were analyzed, thus a comprehensive study on the effect of porous media in micro-combustor is required for the design and practical application of the combustor. Thus, a numerical comparative simulation has been carried out to investigate impacts of key parameters of a micro-combustor with a porous media such as the porous media's length, the porosity coefficient, several types of porous material and inlet velocity on entropy generation, radiation power and its efficiency, wall temperature and inlet temperature, at the same boundary conditions and operation. Moreover, exergy loss and exergy efficiency of micro combustor with porous media was studied. A micro-combustor has been developed to improve the energy and exergy performance as well as to present a comprehensive model for the utilizing porous media in micro-combustor in TPV systems. Ultimately, the most optimal state of micro-combustor to use in TPV systems is introduced for electricity generation.

2. The reference system configuration and its governing equations

In this study, simulation was conducted based on the utilizing porous media with different length inside the micro-combustor and considering the wall temperature rise, the uniform temperature distribution on the wall surface, efficiency increase of first and second laws, and exergy loss reduction. This porous media has several significant characteristics that increase the heat transfer surface inside the micro-combustor, guide hot combustion gases from the center of the tube to the inner wall, and the inner temperature uniformity of the micro-combustor in the porous area. The combustion of H_2/air will be simulated and examined in a three-dimensional and fully turbulent state with 9 species and 19 reactions. The effect of essential parameters, such as the length of the porous media in the micro-combustor, the porosity coefficient of the medium, the thermal conductivity coefficient, inlet velocity, and different heat transfer conditions from the outer wall, on the energy conversion efficiency, heat transfer, exergy efficiency, energy loss, pressure drop, and wall temperature will be examined.

2.1. Mathematical model

Mathematical modeling of hydrogen-air stoichiometric combustion in a micro-combustor, due to the complexity of simulating at the microscale, some assumptions have been considered to simplify the model without insignificant impact on the results. These hypotheses are as follows:

1. Viscosity and weight of the fluid are neglected.
2. Surface reactions are disregarded.
3. Based on the experimental and numerical results obtained by Li et al. [43], the radiation of gases inside the micro-combustor and the inner walls was disregarded. However, the radiation of the outer wall was taken into account.
4. The Mach number is under 0.3 and the mixture of H_2/air is considered an ideal incompressible gas.
5. Viscous force, the radiation of hot gases, and the Duffor's effect due to the low heat flux are ignored.
6. As the Reynolds number of the inlet premixed hydrogen-air is more than 500, the reactive flow is considered as turbulent and at inlet flow is developed

Considering the hypotheses above, conservation of mass, momentum, and energy equations are finally obtained as follows:

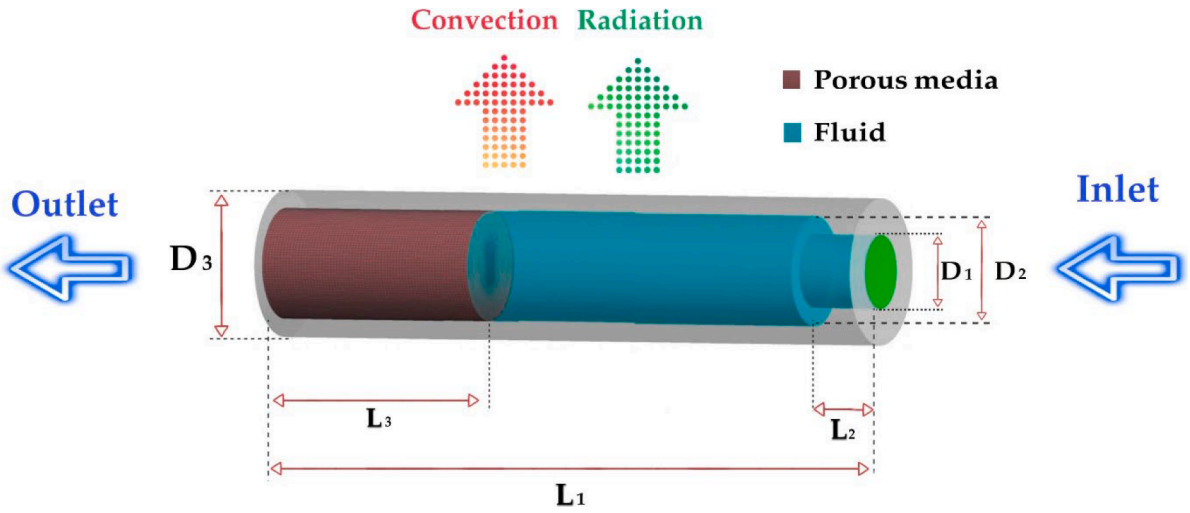

Fig. 2. The geometry of the micro-combustor with a porous medium along with boundary conditions.

$$\nabla(\rho\vec{u}) = 0 \tag{1}$$

$$\rho(\vec{u}.\nabla\vec{u}) = -\nabla P + \nabla.\left(\mu\left[\nabla\vec{u} + (\nabla\vec{u})^{T} - \frac{2}{3}\nabla.\vec{u}I\right]\right) \tag{2}$$

Where ρ denotes the gas density, $\vec{u}$ denotes the velocity vector, P denotes the gas pressure, μ denotes the viscosity, and I denotes a tensor.

$$\nabla.\vec{u}(\rho E_T + P) = \nabla.\left[K_{eff}\nabla T - \left(\sum_j h_j \vec{J}_j\right) + \left(\mu\left[\nabla\vec{u} + (\nabla\vec{u})^{T} - \frac{2}{3}\nabla.\vec{u}I\right]\right).\vec{u}\right] + S_f \tag{3}$$

Where E_T denotes the total energy of the fluid, K_{eff} denotes the effective thermal conductivity coefficient, J_j denotes the diffusion of species j, h_j denotes the entropy of species j, and S_f denotes the entropy generation of the fluid.

The energy equation for the solid area is defined as below [44]:

$$\nabla.(K_s.\nabla T) = 0 \tag{4}$$

Where K_s denotes the thermal conductivity coefficient of the solid area.

The gas equation in an incompressible state is defined as below [45]:

$$P = \rho\frac{R_u}{\overline{W}}T \tag{5}$$

Where $\overline{W}$ is the mean of molecular weight of the mixture gases, and R_u denotes the universal gas constant.

The equation of species transfer is as follows:

$$\nabla.(\rho\vec{u}Y_j) = \nabla\vec{J}_j + \omega_j \tag{6}$$

Where ω_j denotes the reaction rate of species j.

The equation of the entropy transfer is described as below:

$$Tds = du + Pd\left(\frac{1}{\rho}\right) - \sum_{j=1}^{n}\mu_j d\left(\frac{n_j}{\rho}\right) \tag{7}$$

Where s denotes the specific entropy, u denotes the specific internal energy, μ_j denotes the chemical potential of species j, and n_j denotes the number density of species j.

The entropy generation rate $\dot{S}_{gen}$ and irreversibility $\dot{E}_{destructive}$ inside the micro-combustor are defined as follows [44]:

$$\dot{S}_{gen} = \dot{m}(s_{in} - s_{out}) \tag{8}$$

$$\dot{E}_{destructive} = \dot{S}_{gen} \times T_{surr} \tag{9}$$

In accordance with the second law of thermodynamics, the exergy efficiency η_{II} and the exergy loss $\dot{E}x_{loss}$ are defined as follows [44]:

$$\dot{E}x_{loss} = \dot{E}_{loss} + \left[\dot{m} \times T_{surr} \times C_{P_{outlet}} \ln\frac{T_{surr}}{T_{outlet}} - R_{outlet}\ln\frac{P_o}{P_{outlet}}\right] \tag{10}$$

$$\eta_{II} = 1 - \frac{\dot{E}_{destructive} + \dot{E}_{loss}}{\dot{m}_{H2}Q_{LHV}} \tag{11}$$

Where E_{loss} denotes the energy that is transferred outside by exhaust gases, and Q_{LHV} denotes the hydrogen low heat value, which equals 119MJ/kg [17].

Pressure drop inside the micro-combustor is as follows:

$$P_{loss} = P_{inlet} - P_{outlet} \tag{12}$$

Where P_{loss} denotes the pressure drop, P_{inlet} denotes the inlet pressure inside the micro-combustor, and P_{outlet} denotes the outlet pressure equal to 1 atm.

Heat transfer from the outer surface of the micro-combustor $\dot{Q}_{wall}$ occurs through radiative heat transfer $\dot{Q}_{Rad}$ and convective heat transfer $\dot{Q}_{con}$. These two values are calculated using the equations below:

$$\dot{Q}_{wall} = \dot{Q}_{Rad} - \dot{Q}_{con} \tag{13}$$

$$\dot{Q}_{Rad} = e \times \sigma\sum_{i=1}^{n} A_i\left(T_i^4 - T_{surr}^4\right) \tag{14}$$

$$\dot{Q}_{con} = h(T_i - T_{surr}) \tag{15}$$

Where e and σ denote the radiation coefficient of the outer surface of the micro-combustor and the Boltzmann constant, respectively. T_j and A_j indicate the cell temperature of the outer wall and the surface area of the micro-combustor, respectively.

The micro-combustor efficiency η_Q, the radiation efficiency η_{Rad}, and the total efficiency of converting the inlet energy to electric power η_{total}, while using micro-combustors in MTPV power generation systems, are defined as follows:

$$\eta_Q = \frac{\dot{Q}_{wall}}{\dot{Q}_R} \tag{16}$$

$$\eta_{Rad} = \frac{\dot{Q}_{Rad}}{\dot{Q}_R} \tag{17}$$

Table 2
The dimensions of the micro-combustor.

L1	18 mm
L2	2 mm
L3	2,4,8 mm
D1	2 mm
D2	3 mm
D3	4 mm

Table 3
The thermal properties of stainless steel and porous media.

Material name	Density (kg/m^3)	C_p(j/kg.K)	Thermal conductivity (W/m.K)
Stainless steel	8000	503	12
SiC	1300	275	92
Si_3N_4	3210	690	31
Al_2O_3	3970	1000	25
SS304	7930	500	21.5

Table 4
Boundary conditions for the geometry considered in the simulation.

Boundary	Parameters	Values
Inlet	Velocity inlet	5,6,7 m/s
	Pressure outlet	0 Pa
	Turbulent intensity	5 %
	The hydraulic diameter	2 mm and regard to inlet diameter
	Temperature	300 K
Outlet	Pressure outlet	0 Pa
	Turbulent intensity	5 %
	The hydraulic diameter	3 mm and regard to inlet diameter
Inner wall	Interface No-slip	Zero-flux for all species
	Thermal condition	Coupled
	Material	Steel
outer wall	Heat transfer coefficient	5, 10, 15 W/m^2. K
	Emissivity	0.4, 0.6, 0.8

$$\eta_{total} = \eta_{TPV} \cdot \eta_{Rad} \tag{18}$$

Where $\dot{Q}_R$ denotes the heat released from the chemical reaction, and η_{TPV} denotes the efficiency of TPV systems, which stands at 15.4 % [46].

R_T and T_m coefficients are used to describe the wall temperature uniformity and the average wall temperature [14].

$$R_T = \left(\frac{\sum_{i=1}^{n} [|T_i - T_m| A_i]}{T_m \sum_{i=1}^{n} A_i} \right) \times 100 \tag{19}$$

$$T_m = \frac{\sum_{i=1}^{n} T_i A_i}{\sum_{i=1}^{n} A_i} \tag{20}$$

2.2. Geometry configuration

The geometry of the micro-combustor was designed using ANSYS Design Modeler. Three different domains were defined below:

The solid body of the micro-combustor.
The fluid inside the combustor, which includes inlet and combustion gases.
The porous media inside the micro-combustor.

Fig. 2 illustrates a schematic of the geometry of the micro-combustor with a porous media, the fluid inside it, and boundary conditions. Table 2 presents the dimensions observed in the figure. According to Fig. 2, the total length (L1) and the outer diameter (D3) of the micro-combustor are 18 mm and 4 mm, respectively. The inlet diameter (D1) and the step (L2) are both 2 mm. Further, the inner diameter of the micro-combustor and the porous medium diameter (D2) are each 3 mm.

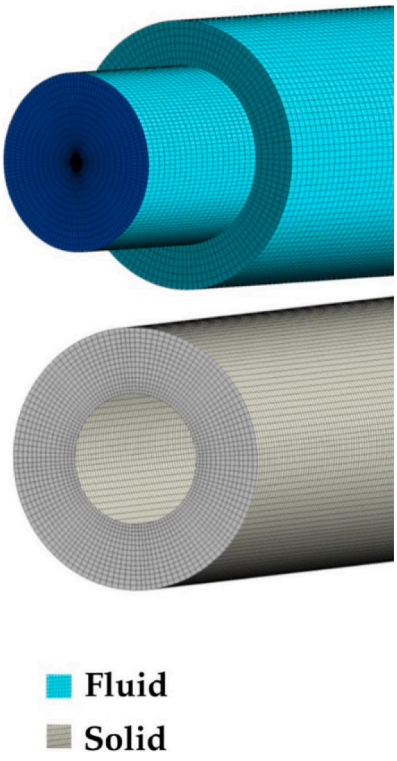

Fig. 3. The grid generation used in the micro-combustor with a porous medium.

The porous medium is fully attached to the micro-combustor. Table 3 illustrates the material and the thermal properties of the porous media used in the micro-combustor [47]. Moreover, Table 4 depicts the boundary conditions concerning the geometry of the micro-combustor.

2.3. CFD simulation and grid independence analysis

The simulation of the micro-combustor has been carried out in Fluent R2 2019. The $k-\epsilon$ model, which has the highest compatibility with the experimental results [48], has been utilized for turbulence model. The turbulent chemical reaction rate is calculated through emissivity [23]. A second-order discretization is conducted for all the equations, and the coupled method is used for the pressure–velocity coupling [49]. H_2/air combustion reactions with 19 micro-reactions and 9 species are used in simulation [50]. The convergence criteria for the mass, momentum, and species transfer equations are from the 1×10^{-3} order while the convergence criteria for the energy equation is from the 1×10^{-6} order.

A structured grid for the solid, porous media and fluid domains of the micro-combustor were generated, as can be seen in Fig. 3. The total 622,000 elements were generated during the meshing. In addition, the mesh size of 0.1 mm is employed for all the cases.

Grid independence for the micro-combustor with and without a porous medium was analyzed to ensure the results are grid independent and to find the minimum number of required elements. Four different meshes with 999000, 622000, 211000, and 112000 elements were examined to find the minimum number of required elements to analyze the effect of the micro-combustor's dimensions on its performance. Fig. 4 illustrates the temperature distribution of these four meshes. According to Fig. 4, the wall temperature does not change with an increase in the number of elements from 622000. Moreover, the wall temperature profile for meshes with 999000 and 622000 elements match each other. As can be seen in Fig. 4, the temperature distribution graph has two temperature peaks: the first is at the step and is due to the combustion reaction and drastic increase in the temperature of the inlet gases, and the second peak is caused by the start of the area with a

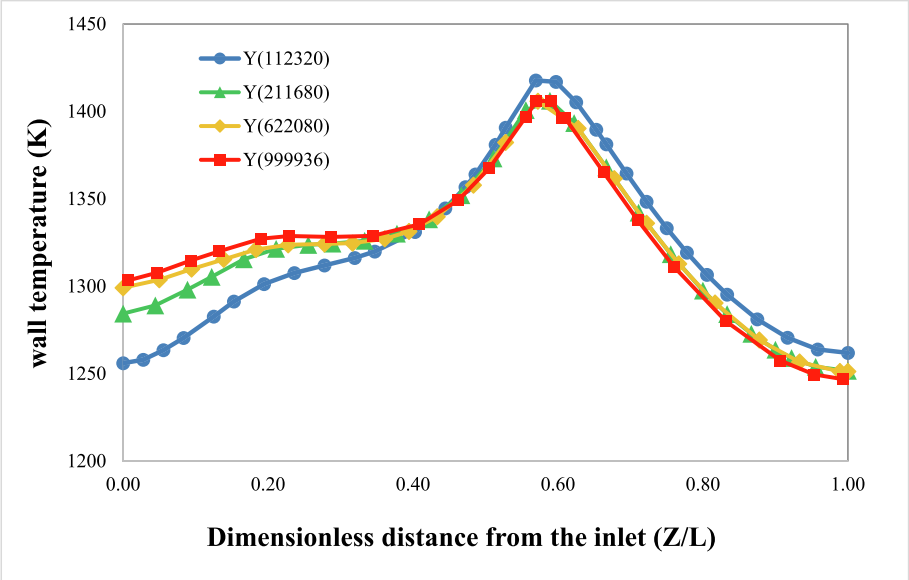

Fig. 4. Grid independence analysis for a micro-combustor with a 8 mm-long porous medium.

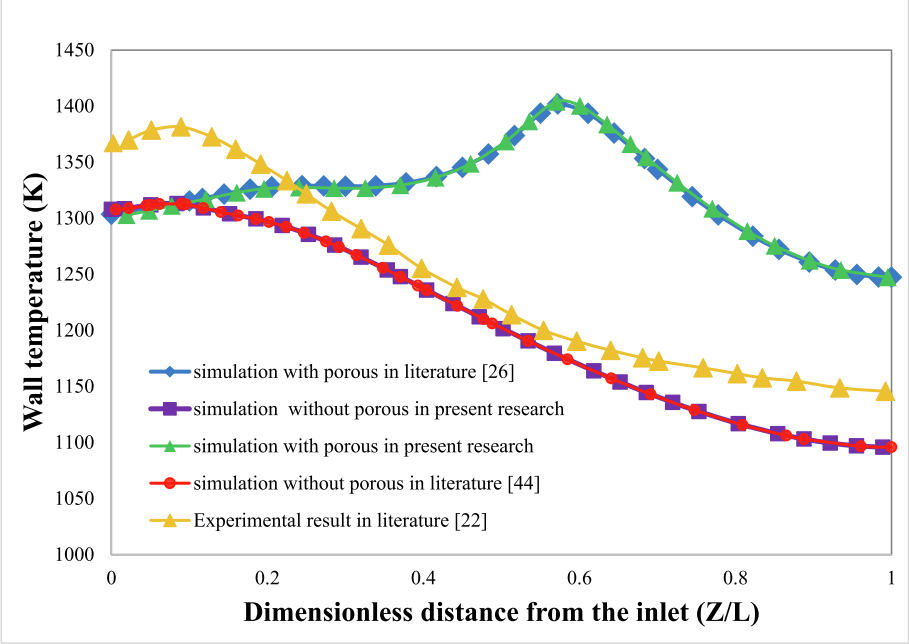

Fig. 5. Comparing changes in the wall temperature of the system in the present study with the experimental and numerical results of other studies.

porous medium. Fig. 4 shows at the entrance of the inlet, there is a temperature discrepancy for grids with a low number of different elements. However, this discrepancy increases as the distance from the inlet of the micro-combustor grows. Furthermore, the wall temperature sensitivity at the end of the micro-combustor with a porous medium is high compared to the number of elements. A rise in the number of elements for a similar situation z/l would decrease this discrepancy in a way that the maximum wall temperature discrepancy for z/l is the same and the number of 211000 and 622000 meshes is 9 K. As the number of elements increases from 622000, the wall temperature does not change. For instance, the temperature distribution in a grid with 999000 elements are close with a grid 622000 elements and only 1.5 % difference for the wall temperature. Therefore, in the present study, the meshing with 622000 elements for the micro-combustor with a porous medium is deployed for the entire simulation.

2.4. Validation

To validate the numerical modelling, the wall temperature graph of the micro-combustor without a porous medium will be compared with the experimental results of Yang et al. [26] and the numerical simulation of Yilmaz et al. [51]. Also, the wall temperature graph of the micro-combustor with a porous medium will be compared with the results of the numerical simulation of Mohseni et al. [30] at the inlet velocity of 5 m/s and the equivalence ratio of 1.0. As can be observed in Fig. 5, the calculated wall temperature of the micro-combustor without/with a porous medium is the same as the simulation results of Yilmaz with a tube combustor. The greatest discrepancy was in the temperature peak at 1 %, which decreases along the micro-combustor. The difference between the numerical simulation of Yilmaz et al. [51] and the experimental results are due to using a micro-combustor with a rectangular

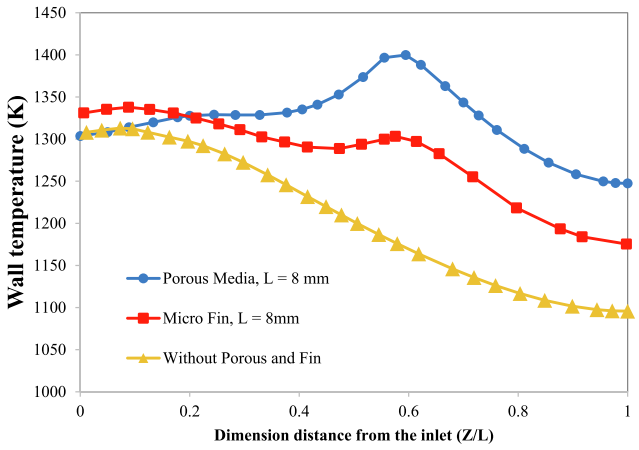

Fig. 6. Changes in the wall temperature of the system per distance from the inlet of the micro-combustor in three states: with a medium, with a micro-fin, simple [48].

cross-section in the experiment setup. Thus, the results obtained from the simulation are reliable. The results in Fig. 5 illustrate the validity of this model in examining the effect of the porous medium on the thermal performance and energy of the micro-combustor.

3. Results and discussions

3.1. Analyzing the thermal performance and the efficiency of the Micro-Combustor under different physical circumstances

Fig. 6 depicts the graph of the outer wall temperature of a micro-combustor with an 8 mm porous medium and a porosity coefficient of 0.9, a micro-combustor with an 8 mm-long micro-fin (according to reference [48]), and a simple micro-combustor. The graph in Fig. 7 illustrates parameters including uniformity coefficient, maximum temperature, minimum temperature, average outer wall temperature, and exhaust gas temperature in the micro-combustor with a porous medium, with a micro-fin, and in a simple state. Fig. 7 shows the significant performance of the micro-combustor with a porous medium and the micro-combustor with a micro-fin compared to the simple system. In the case of the simple micro-combustor, the uniformity coefficient R_t equals 4.58. In TPV systems, the low values for the uniformity coefficient are more favorable as a reduction in this coefficient causes more temperature uniformity in the outer wall, increasing the system's lifetime. According to Fig. 7, the values of this coefficient for the micro-combustor with a porous medium and the micro-combustor with a micro-fin stand at 2.27 and 1.75, respectively, indicating the significant temperature uniformity of the outer wall.

Temperature uniformity of the outer wall, exergy efficiency, and high radiation efficiency are regarded as some of the most significant necessities in using the micro-combustor of TPV systems. As illustrated in Fig. 8, using a porous medium and setting a micro-fin in the micro-combustor of TPV systems dramatically increases the exergy efficiency and radiation efficiency. Hence, it can be concluded that it is crucial to use a porous medium or a micro-fin in the micro-combustor as not only does it make the outer wall temperature more uniform and increases the system's lifetime, but it also increases exergy efficiency and radiation efficiency. A comparison of these three states in the graph in Fig. 8 reveals that the porous medium performs better than the micro-fin in terms of radiation and exergy efficiency. Accordingly, radiation and exergy efficiencies for an 8 mm-long porous medium are 52.91 % and 44.5 %, respectively, which is higher by 3.51 % and 3.9 % than the one with a micro-fin and 15.61 % and 20.8 % than the one without a medium. Additionally, during the analysis of different circumstances of using a porous medium, the most optimum way of using it in TPV systems will be examined to obtain the highest exergy efficiency and radiation efficiency and the lowest uniformity coefficient on the surface of the outer wall of the micro-combustor.

3.2. Analyzing the effect of changes in the porous medium length on the Micro-Combustor

This section will analyze the effect of changes in the porous medium length in the micro-combustor on its performance, maximum temperature, minimum temperature, average outer wall temperature, and exhaust gas temperature, uniformity coefficient, temperature contour at a plane of symmetry, and various cross-sections along the micro-combustor with a porous medium and the contour of OH mass fraction distribution.

In cylindrical micro-combustors, the temperature and velocity of exhaust gases increase from the inner wall to the center of the cylinder while the outer wall temperature along the micro-combustor without a

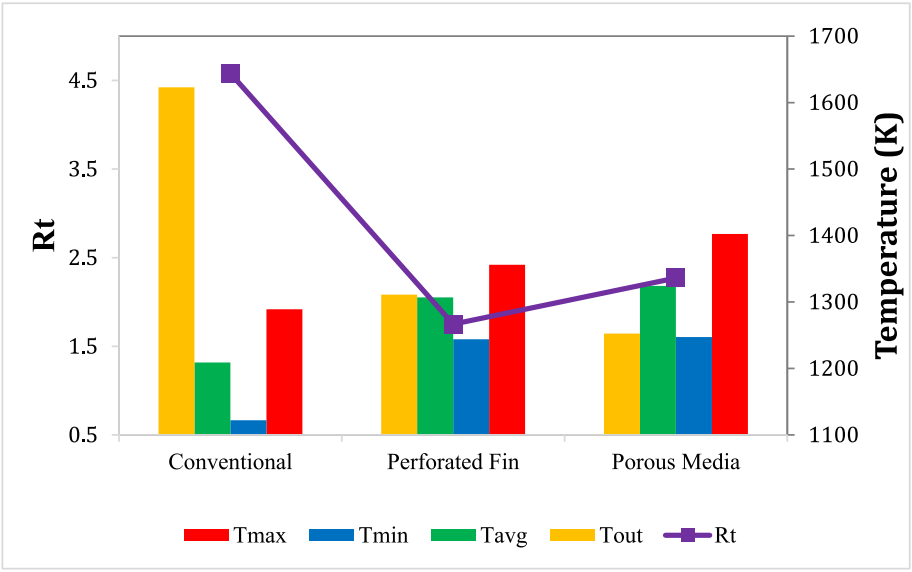

Fig. 7. Uniformity coefficient, maximum temperature, minimum temperature, average outer wall temperature, and the temperature of exhaust gases in the micro-combustor with a porous medium, with a micro-fin, and in a simple state.

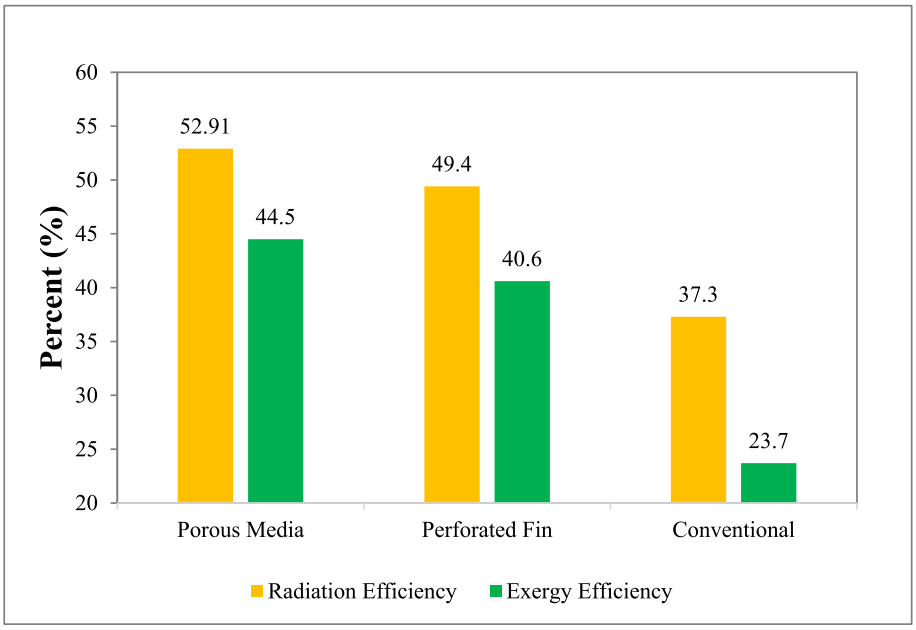

Fig. 8. Changes in radiation efficiency and exergy efficiency in the micro-combustor with a porous medium, with a micro-fin, and in a simple one.

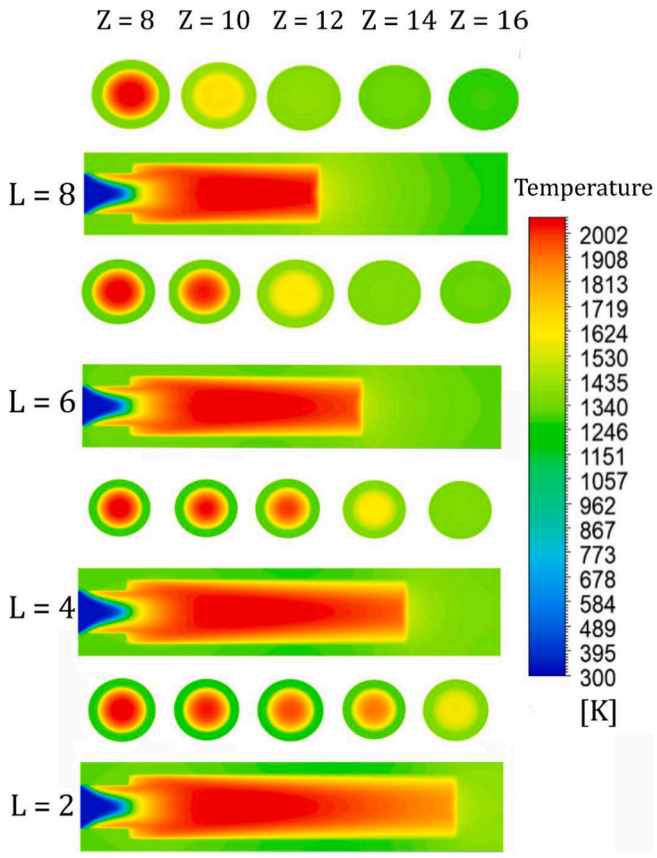

Fig. 9. Temperature contour at the plane of symmetry and various cross-sections along the micro-combustor with porous media of $L = 2, 4, 6, 8mm$.

porous medium, especially at the outlet, decreases. However, the temperature of exhaust combustion gases is much higher than the wall temperature, which causes energy and exergy loss. Therefore, to enhance the performance of the cylindrical micro-combustor, a new porous medium, as illustrated in Fig. 9, is utilized. Fig. 9 shows temperature distribution at the plane of symmetry and various cross-sections along the micro-combustor with a porous medium of different lengths $L = 2, 4, 6, 8mm$. This type of porous medium inside the micro-combustor increases the heat transfer surface and moves hot gases from the center of the cylinder to the walls of the micro-combustor. Additionally, it makes temperature distribution in the inner area with a porous media more uniform than the one without a porous media. The temperature of exhaust gases drops along the micro-combustor due to an increase in heat transfer, which results in exergy and energy loss reduction at the outlet.

Fig. 10 shows temperature changes in the outer wall of the micro-combustor with and without a SiC porous medium (whose properties are shown in Table 3) with a 0.9 porosity coefficient and at a 5 m/s velocity. As depicted in Fig. 10, using a porous medium drastically increases wall temperature in a way that selecting an 8 mm-thick porous medium increases the average temperature by 115 K, making its final value reach 1324 K. Also, the average temperature for the 6 mm length increases by 111 K, making its final value reach 1320 K. According to the equation of radiation in the outer wall (Equation (14)), this temperature rise also the radiation power. Additionally, the porous medium makes the wall temperature more uniform and increases the efficiency of TPV systems. According to Fig. 11, the R_t coefficient, as a criterion for determining the uniformity of the wall temperature, equals 2.27 for an 8 mm-long porous medium while it equals 1.29, 1.7, and 2.32 for lengths of 6 mm, 4 mm, and 2 mm, respectively. As can be observed in Fig. 11, the R_t coefficient for a 6 mm-long porous medium reaches its lowest point, making the discrepancy between the maximum and the minimum temperatures stand at 121 K, which is equivalent to the most uniform temperature on the wall surface. As illustrated in Fig. 10, the temperature graph shifts from one peak in the state without a medium to two temperature peaks in the state with a porous medium, and increased dimensions of the medium increase the average temperature. Nonetheless, the discrepancy between the maximum and the minimum temperatures and the uniformity coefficient of the wall temperature increase with an increase in the dimensions of the medium, which reduces the system's lifetime and increases its susceptibility.

Based on Fig. 12, temperature decreases along the centroidal axis with an increase in the length of the porous media. By assuming the porous medium to be 6 mm long, heat transfer from the inside to the outside, at a 0.66 dimensionless distance from the inlet, increases while

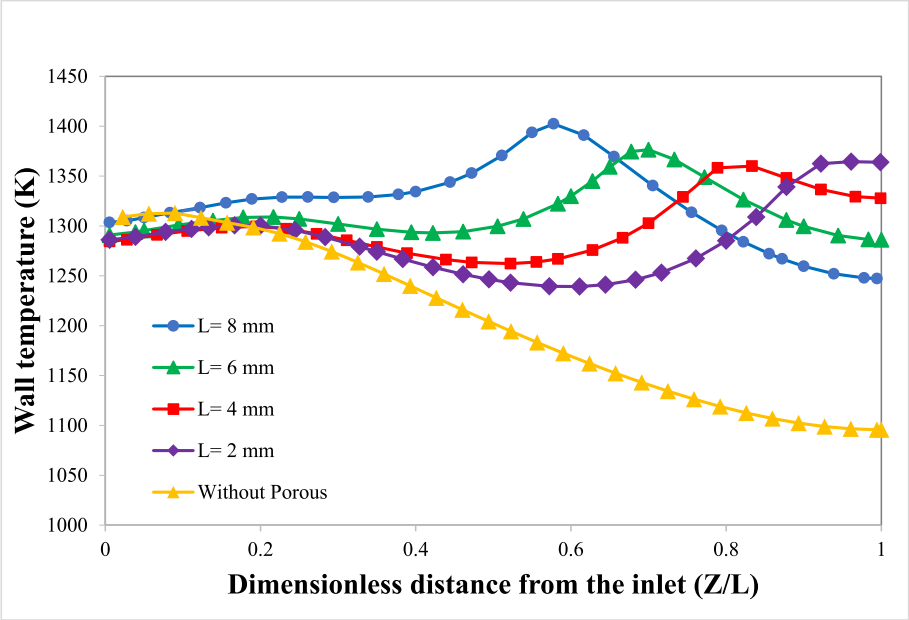

Fig. 10. Temperature profile of the micro-combustor with and without porous media of $L = 2, 4, 6, 8mm$.

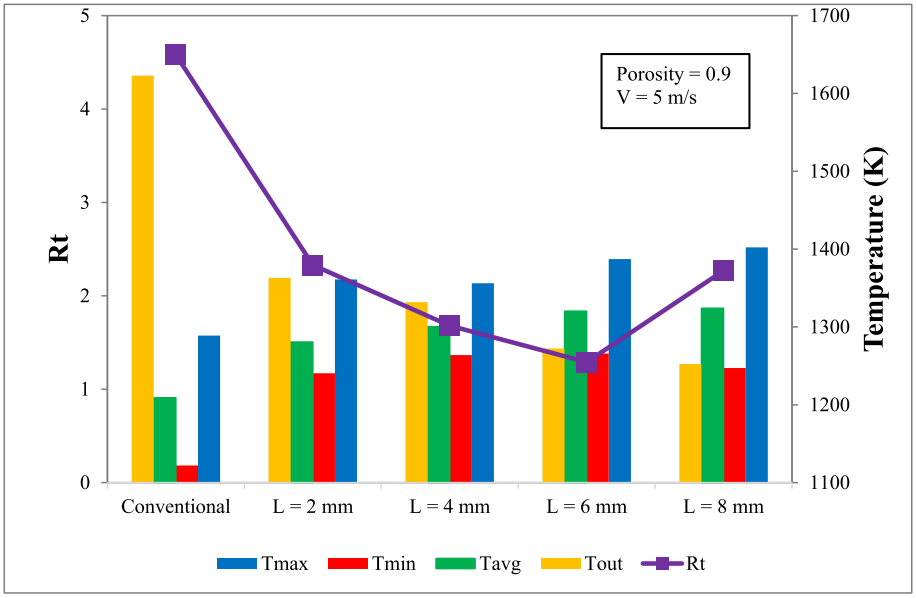

Fig. 11. Changes in the uniformity coefficient, maximum temperature, minimum temperature, average outer wall temperature, and the temperature of exhaust gases in the micro-combustor with or without porous media of $L = 2, 4, 6, 8mm$.

the temperature of the central line decreases. Additionally, the temperature of combustion gases, at dimensionless distances farther from the inlet, is higher, meaning the temperature along the centroidal axis of the shorter porous medium is higher. Temperature drop in combustion inside the micro-combustor reduces NO_x.

3.3. Analyzing the effect of changes in the porous medium thickness on radiation efficiency and exergy of the Micro-Combustor

Radiation power, exergy efficiency, and high radiation efficiency are regarded as some of the most significant necessities in using the micro-combustor of TPV systems. To achieve this goal, wide surfaces were used to increase the inner heat transfer surface. For instance, in the state with a porous medium, the inner surface area subjected to heat transfer is greater than one without. This is due to the high porosity percentage of the one with a porous medium, which increases heat transfer in TPV systems. Fig. 13 shows changes in exergy efficiency and exergy loss while Fig. 14 shows radiation efficiency and radiation power at a 5 m/s inlet velocity and a 0.9 porosity coefficient for various porous media lengths.

Using a porous medium significantly increases radiation and exergy efficiencies compared to the one without a medium. Accordingly, radiation and exergy efficiencies for an 8 mm-long medium are 52.91 % and 44.5 %, respectively, which is higher by 15.6 % and 20.8 %, respectively, than the one without a medium. An increase in the length of the porous medium also increases exergy efficiency, radiation efficiency, and the micro-combustor efficiency η_Q. According to Fig. 14, the radiation power is directly proportional to the length of the porous medium of the micro-combustor so that greater radiation power is achieved with greater lengths. The reason behind this matter is related to Equation (14)

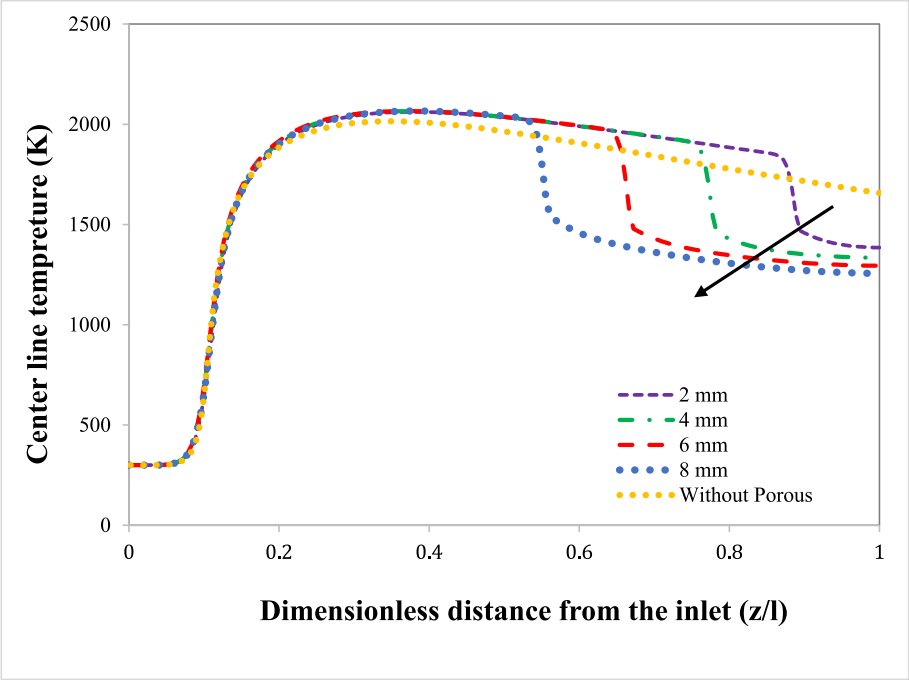

Fig. 12. Temperature profile of the center of the micro-combustor with and without porous media of $L = 2, 4, 6, 8mm$.

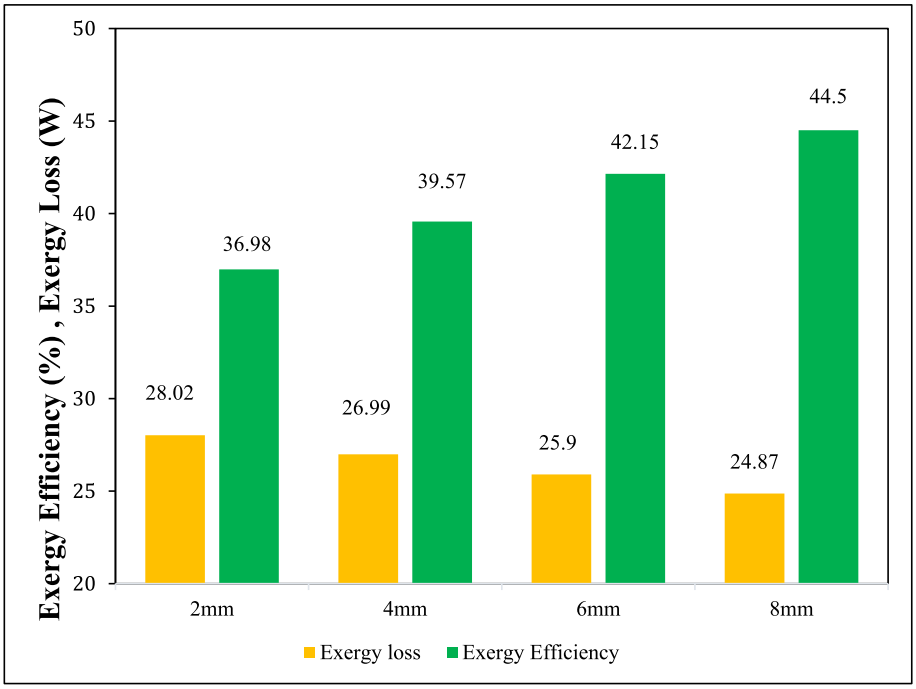

Fig. 13. Exergy loss and exergy efficiency in the micro-combustor with porous media of various lengths.

in which the radiation power is directly proportional to the outer surface of the wall.

Radiation efficiency from the outer wall of different micro-combustors is defined as the ratio of energy emitted by the outer wall to total inlet energy. An increase in the length of the porous medium in the micro-combustor also increases the energy conversion efficiency. The highest radiation efficiency is from the micro-combustor with an 8 mm-long porous medium, which is greater than the micro-combustor with a 6 mm porous medium by approximately 1.8 %. Therefore, an increase in the length of the porous medium of the micro-combustor has a marginal effect on the improvement of radiation efficiency. Furthermore, the radiation efficiency difference between the smallest and the biggest porous media of the micro-combustor (2 mm and 8 mm) stands at only 5.77 %.

3.4. Analyzing the effect of changes in the inlet velocity on the thermal Performance, exergy Efficiency, and radiation efficiency of the Micro-Combustor

Fig. 15 shows changes in the wall temperature at different velocities

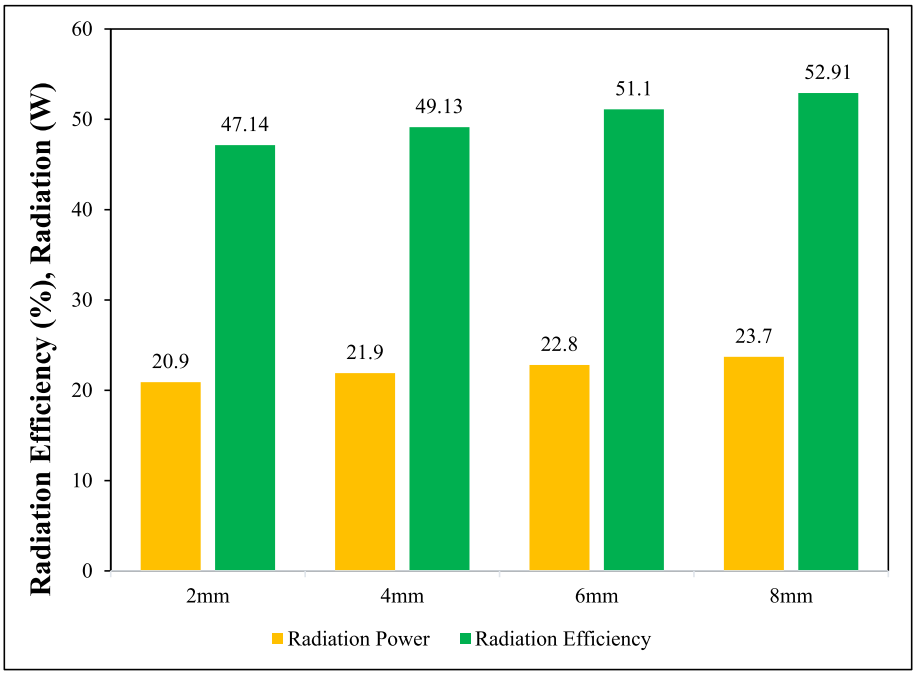

Fig. 14. Radiation power and radiation efficiency in the micro-combustor with porous media of various lengths.

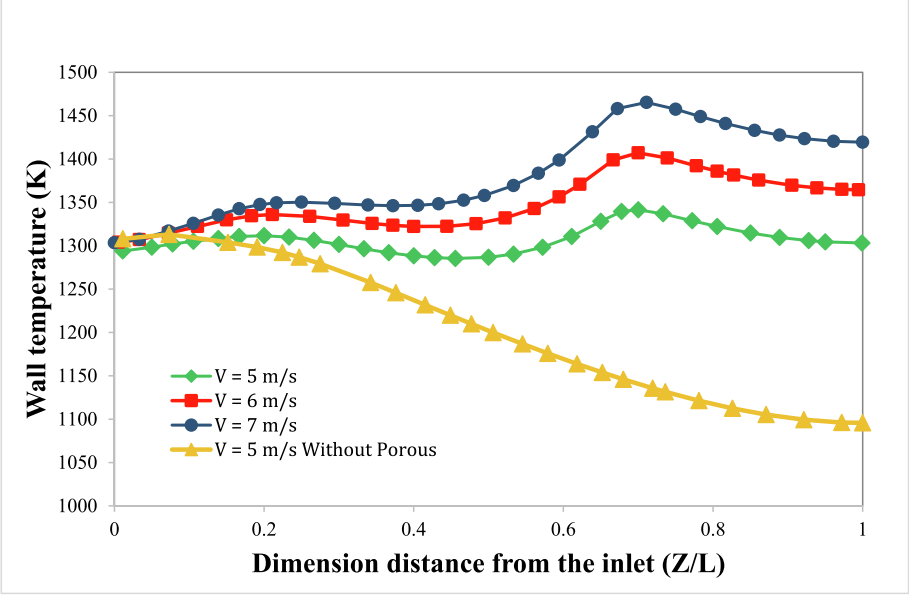

Fig. 15. Wall temperature of the micro-combustor with a porous medium at different inlet velocities.

for the micro-combustor with a 6 mm-long porous medium and a 0.5 porosity coefficient. Fig. 16 also illustrates the effect of the inlet velocity on the uniformity coefficient, maximum temperature, minimum temperature, average outer wall temperature, and temperature of exhaust gases of the micro-combustor with a porous medium. Based on Fig. 15, increased inlet velocity causes the average wall temperature to rise and its uniformity to decrease. Accordingly, for maximum velocity $V = 7\frac{m}{s}$, according to Fig. 16, the difference between the maximum and minimum temperatures is 162 K and the *Rt* coefficient is 3.24, which is not considered a favorable value for the uniformity coefficient. Additionally, the discrepancy between the maximum and minimum temperatures and the uniformity coefficient at minimum velocity (5 m/s) stands at 56 K and 0.89, respectively, indicating an extremely uniform temperature on the wall.

Fig. 17 shows changes in the radiation efficiency and exergy efficiency in the micro-combustor with a 6 mm porous medium at different inlet velocities. As depicted in the figure, the increase of exhaust gases temperature at a high velocity reduces radiation efficiency and exergy efficiency so that radiation and exergy efficiency discrepancies between the maximum and minimum velocities stand at 4.44 % and 7.87 %, respectively.

Fig. 18 shows the contour of the OH mass fraction and its gradient at the plane of symmetry for the minimum and maximum porous media lengths and inlet velocity in the dimensionless state. According to Fig. 18, a reduction in the thickness of the porous medium and an increase in the inlet velocity of the micro-combustor increases the OH expansion in the micro-combustor. Moreover, the OH mass fraction at the inlet of the micro-combustor at low velocity and great length is

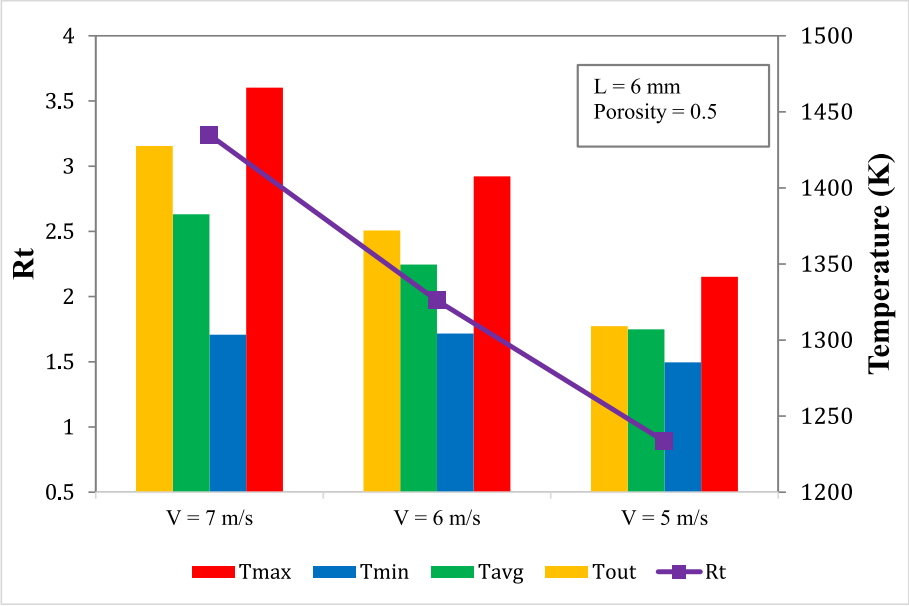

Fig. 16. Changes in uniformity coefficient, maximum temperature, minimum temperature, average outer wall temperature, and temperature of exhaust gases in the micro-combustor with a porous medium at different inlet velocity.

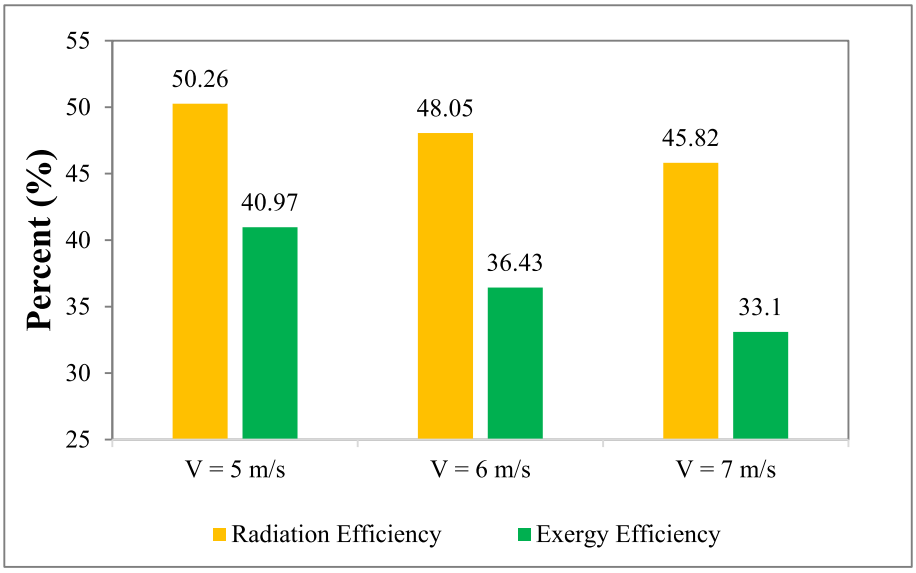

Fig. 17. Radiation efficiency and exergy efficiency in the micro-combustor with a 6 mm-thick porous medium at different inlet velocities.

greater than this value at high velocity and small length. This causes the flame to move from the inlet to the inner area of the micro-combustor and the maximum wall temperature to transfer to the outlet, which results in the uniformity of the wall temperature.

3.5. Analyzing the effect of changes in the porosity coefficient on the thermal Performance, exergy Efficiency, and radiation efficiency of the Micro-Combustor

Based on the previous topics, it was determined that the most viable performance, including the favorable efficiency and temperature distribution uniformity, occurs when a 6 mm-long porous medium at the inlet velocity of 5 m/s is used in the micro-combustor. Later, the effect of the porosity coefficient of porous media on the performance of the micro-combustor with a medium will be examined. Parameters including maximum temperature, minimum temperature, average outer wall temperature, the temperature of exhaust gases, and uniformity coefficient of different porosity coefficient values will be calculated and the outputs such as radiation efficiency and exergy efficiency, will be examined to analyze the effect of changes in the porosity coefficient of porous media in the micro-combustor on its performance.

An increase in porosity coefficient also increases the number of porous particles in the object, and consequently moving fluid through pores become restricted, which results in slow fluid movement and temperature increase. Fig. 19 illustrates changes in the temperature profile of the micro-combustor with different values of porosity coefficient and per dimensionless distance from the inlet of the micro-combustor. As depicted in the figure, despite increased wall temperature due to a rise in porosity coefficient, the discrepancy of maximum and minimum temperatures in the wall also rises, which causes the uniformity coefficient to go up. This is also clear in Fig. 20 at the 5 m/s inlet velocity and the 6 mm length in a way that an increase in porosity

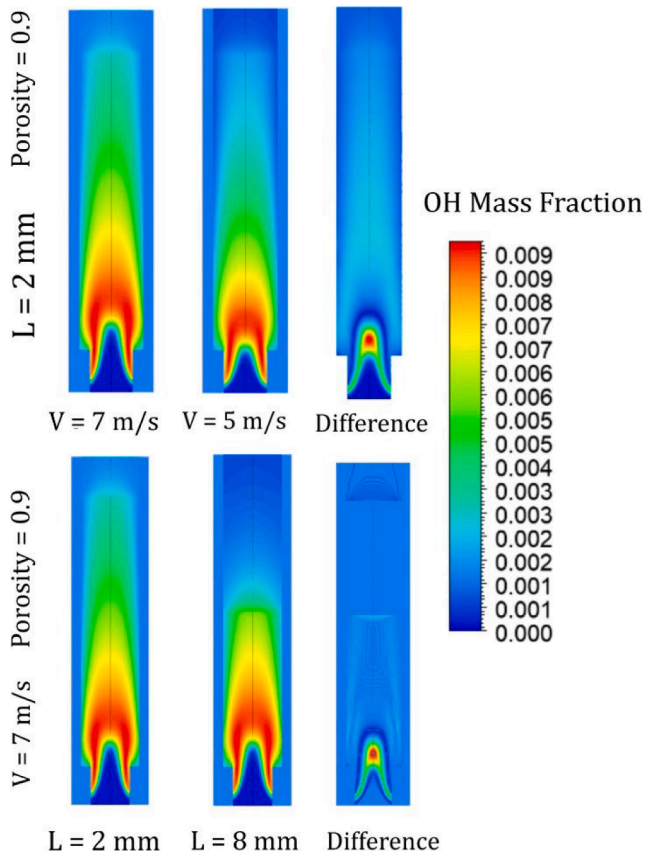

Fig. 18. Changes in the mass fraction of OH at the plane of symmetry for inlet velocities and different length of porous media.

coefficient from 0.5 to 0.9 leads to an increase in uniformity coefficient from 0.89 to 1.29.

Fig. 21 illustrates changes in radiation efficiency and exergy efficiency as a function of the porosity coefficient. According to Fig. 21, radiation efficiency and exergy efficiency are directly proportional to the porosity coefficient of the micro-combustor so that maximum efficiency is obtained with the maximum porosity coefficient in the micro-combustor. This is because as the contact between the moving fluid and the pores increase, heat transfer enhances due to an increase in the porosity coefficient.

According to Fig. 21, maximum radiation efficiency and exergy efficiency belong to the micro-combustor with a 0.9 porosity coefficient, which shows a marginal rise at approximately 0.84 % and 1.18 % compared with the 0.5 porosity coefficient. This indicates that radiation efficiency and exergy efficiency are less susceptible to changes in the porosity coefficient of the micro-combustor. However, it is more favorable to select smaller values of the porosity coefficient as, according to Fig. 21, an increase in the porosity coefficient from 0.5 to 0.9 increases the uniformity coefficient from 0.89 to 1.29.

3.6. Analyzing the effect of changes in the material of a porous medium in the Micro-Combustor

Based on the previous topics, using a 6 mm-long porous medium with a 0.5 porosity coefficient and a 5 m/s inlet velocity showed the most viable performance in terms of uniformity coefficient, radiation efficiency, and exergy efficiency in micro-combustors with porous media.

Later, four different materials of porous media, whose properties are depicted in Table 3, will be discussed to find the most proper porous medium for the micro-combustor.

Fig. 22 shows changes in radiation efficiency and exergy efficiency in the micro-combustor with 6 mm-long porous media of different materials with an inlet velocity of 5 m/s. According to Fig. 22, using the porous SS304 creates maximum radiation efficiency and exergy efficiency in the micro-combustor. However, the performance of this material is not significantly different from other porous media with a discrepancy of less than 1 % for both efficiencies compared with other media (Fig. 22).

3.7. The effect a porous medium and its dimensions on pressure drop

Increased pressure drop is one of the defects of using porous media. Fig. 23 depicts pressure drop for porous media of different lengths and the inlet velocity of 5 m/s along the centroidal axis. Pressure drastically drops from the inlet to the step, maintains relatively constant from the step to the outset of the porous medium but then significantly decrease in porous media. Moreover, pressure is at maximum at the outset of the porous medium, and pressure on the porous media has a linear drop at the outset of the medium. Further, the pressure gradient from the outset to the end of the porous media decreases as the length increases. An

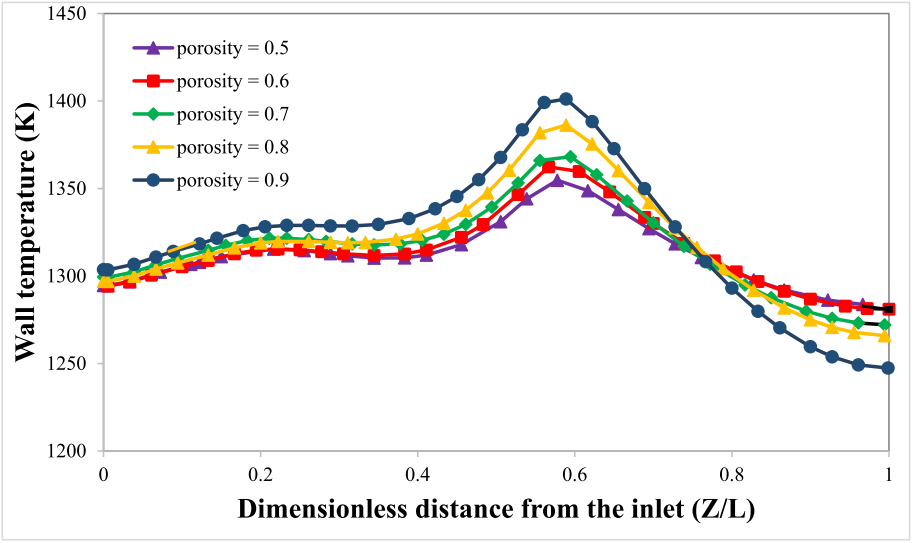

Fig. 19. Changes in the wall temperature for different values of porosity coefficient of the micro-combustor with a 6 mm-long porous medium and at a 5 m/s inlet velocity.

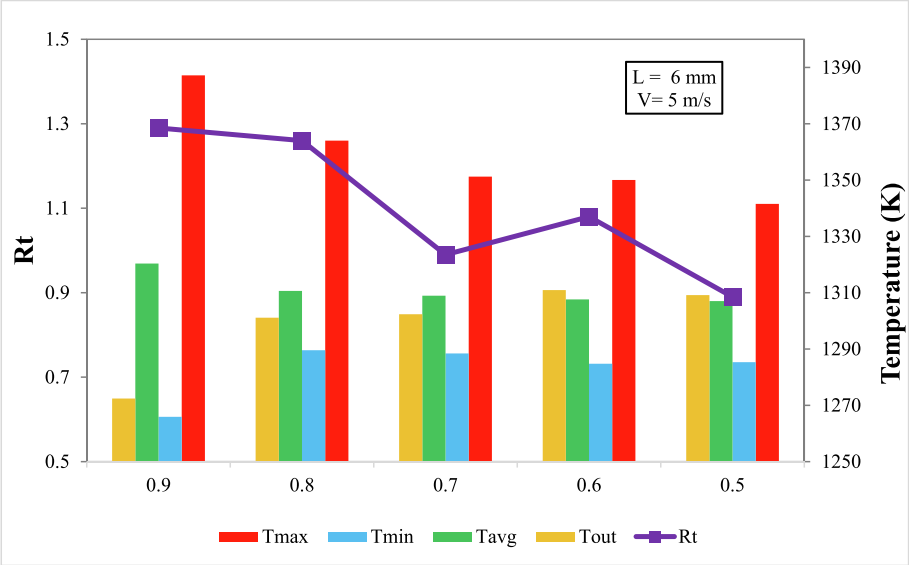

Fig. 20. Changes in uniformity coefficient, maximum temperature, minimum temperature, average outer wall temperature, and temperature of exhaust gases in the micro-combustor with a 6 mm-long porous medium and at a 5 m/s inlet velocity for different values of porosity coefficient.

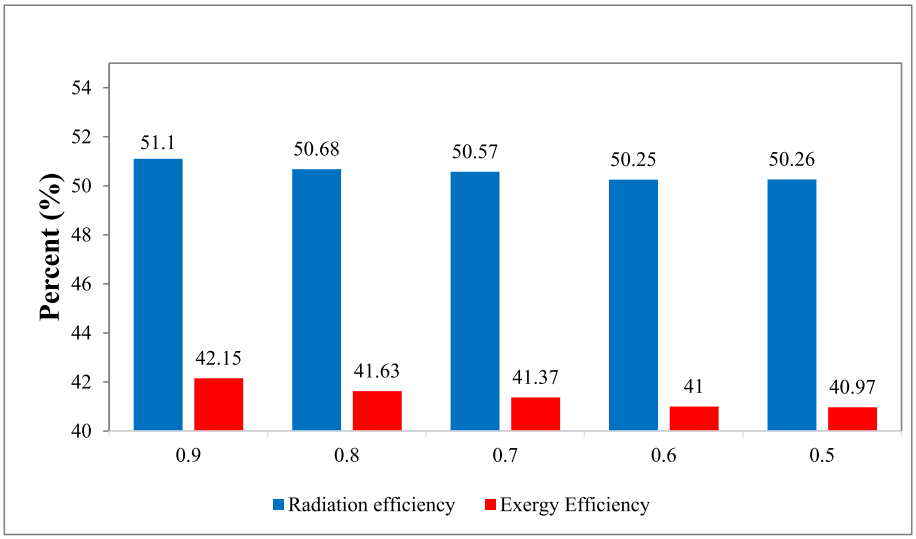

Fig 21. Radiation efficiency and exergy efficiency in the micro-combustor with a 6 mm-long porous medium, at a 5 m/s inlet velocity, and with different porosity coefficients.

increase in the length of the porous medium also increases friction, which intensifies pressure drop so that with a 2 times increase in the length of the porous medium from 4 mm to 8 mm, pressure drop increases by 238 Pa.

3.8. Using the Micro-Combustor with the suggested porous medium for TPV systems

Table 5 presents essential parameters for the design and utilization of a micro-combustor with a porous medium. The most significant parameters include radiative heat transfer, energy and exergy efficiencies of the TPV system are shown in this table. For different values of the studied parameters such as different thermal conductivity coefficients, convective thermal transfer, and radiation intensity coefficient are the total efficiency obtained. Finally, for the micro-combustor in the present model, the maximum efficiency of total electricity generation is 12.75 %.

4. Conclusion

In this study, to enhance the performance and improve the micro-combustor for utilization in Thermo-Photovoltaic systems was studied through a 3D CFD simulation. The effect of different parameters in porous media micro combustor on the energy and exergy efficiencies entropy generation average wall temperature and its uniformity, inlet mass flow, heat transfer, energy efficiency and exergy efficiency were analyzed. The main findings are summarized as follows:

- The porous medium showed a favorable effect on the performance of the micro-combustor, especially on exergy and energy efficiency, temperature of the outer wall, and uniform distribution of temperature.
- Generally, an analysis on different models revealed that uniform temperature distribution is more important than exergy and radiation efficiency. Further, it has a decisive role in the performance of Thermo-Photovoltaic systems.

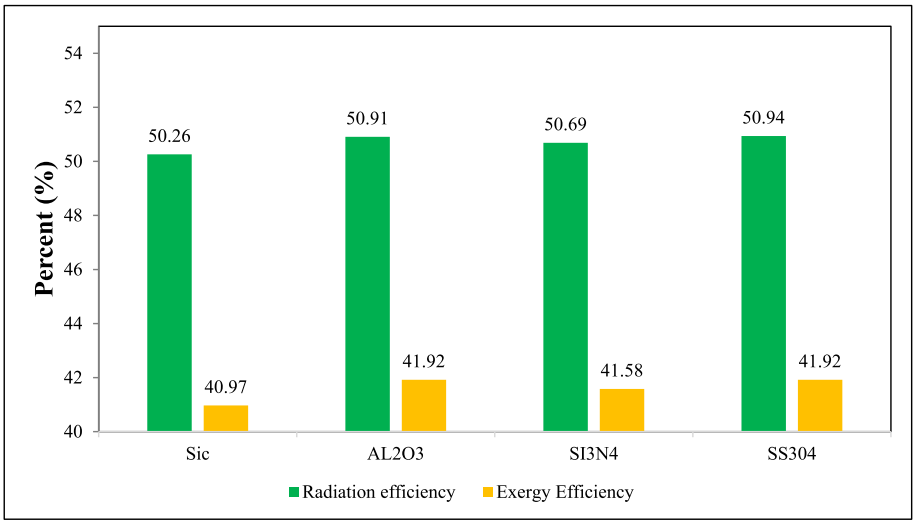

Fig. 22. Changes in radiation efficiency and exergy efficiency in the micro-combustor with a 6 mm-long porous medium at the inlet velocity of 5 m/s of different materials.

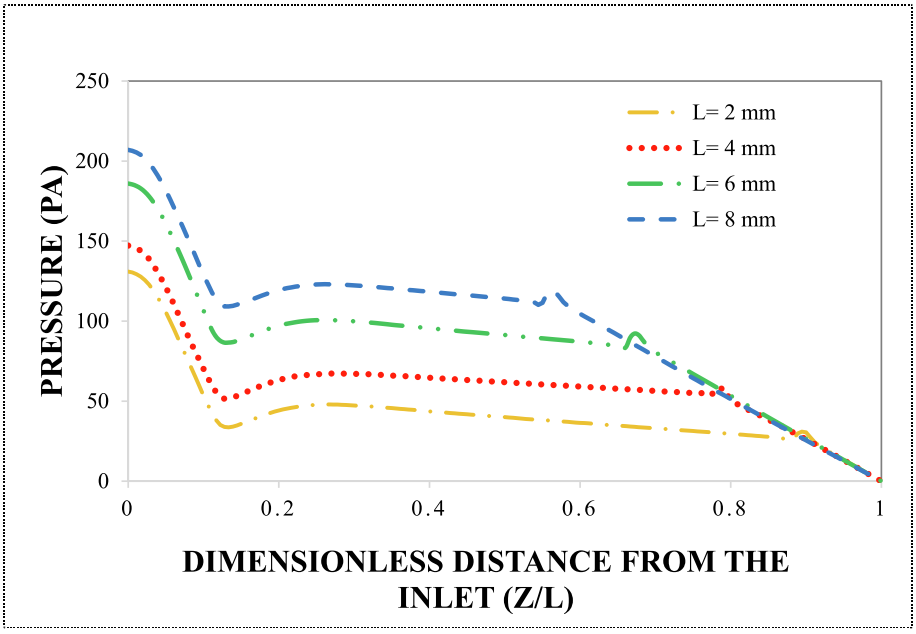

Fig. 23. Pressure drops along the Centroidal axis of the micro-combustor with porous media of.$L = 2, 4, 6, 8\,m$

- it was found that the micro-combustor with a 6 mm-long porous medium has the least temperature uniformity coefficient and great exergy efficiency and radiation efficiency. As a result, it shows the most favorable performance in the utilization of porous media in a micro-combustor.
- Under the same conditions, the highest average wall temperature and the highest uniformity coefficient of wall temperature were obtained for the micro-combustor with an 8 mm-long porous medium. Moreover, a decrease in the length of the porous medium in the micro-combustor leads to an increase in the exergy efficiency and a decrease in the exergy loss.
- Using a 6 mm-long porous medium increases the average wall temperature by 111 K compared with the case without a porous medium. Moreover, the uniformity coefficient of wall temperature decreases from by 80.05 %, from 4.58 to 0.89. As a result, using porous media increases temperature distribution uniformity on the surface of the wall compared to the case without a medium.
- A 6 mm-long porous medium increases the radiation efficiency and exergy efficiency by 37 % and 79.7 % compared to the micro-combustor without a porous medium. Total efficiency in the conversion of inlet energy to electric power increases from 8.9 % to 12.32 %.

Declaration of Competing Interest

The authors declare that they have no known competing financial interests or personal relationships that could have appeared to influence the work reported in this paper.

Data availability

Data will be made available on request.

Table 5
Main parameters for the design and utilization of the micro-combustor with a porous medium.

L	Porosity	V	$\dot{Q}_{Rad}$	η_{Rad}	η_{II}	η_{Q}	η_{total}
8	0.9	5	23.7	**52.91**	**44.51**	24.1	**12.75**
8	0.9	6	27.3	50.84	40.33	24.1	12.25
8	0.9	7	**30.5**	48.98	37.14	24.1	11.80
8	0.8	5	23.4	52.14	43.63	24.1	12.57
8	0.8	6	26.9	50.29	39.41	24.1	12.12
8	0.8	7	30.0	48.40	36.57	24.1	11.67
8	0.7	5	23.2	51.75	43.05	24.1	12.47
8	0.7	6	26.7	49.87	38.82	24.1	12.02
8	0.7	7	29.7	47.96	35.78	24.1	11.56
8	0.6	5	23.0	51.36	42.63	24.1	12.38
8	0.6	6	26.4	49.46	38.36	24.1	11.92
8	0.6	7	29.4	47.54	35.33	24.1	11.46
8	0.5	5	22.8	51.15	42.27	24.1	12.33
8	0.5	6	26.2	49.23	38.04	24.1	11.86
8	0.5	7	29.2	47.28	34.99	24.1	11.40
6	0.9	5	22.9	51.11	42.16	24.1	12.32
6	0.9	6	26.2	48.91	37.67	24.1	11.79
6	0.9	7	29.0	46.93	34.53	24.1	11.31
6	0.8	5	22.7	50.69	41.64	24.1	12.22
6	0.8	6	26.0	48.72	37.44	24.1	11.74
6	0.8	7	28.8	46.61	34.10	24.1	11.23
6	0.7	5	22.5	50.58	41.37	24.1	12.19
6	0.7	6	25.8	48.40	36.85	24.1	11.66
6	0.7	7	28.6	46.33	33.73	24.1	11.16
6	0.6	5	22.4	50.25	41.00	24.1	12.11
6	0.6	6	25.7	48.20	36.74	24.1	11.62
6	0.6	7	28.4	46.16	33.48	24.1	11.13
6	0.5	5	22.4	50.27	40.98	24.1	12.11
6	0.5	6	25.5	48.05	36.43	24.1	11.58
6	0.5	7	28.2	45.83	33.10	24.1	11.04
4	0.9	5	22.0	49.19	39.57	24.1	11.85
4	0.9	6	24.9	46.77	34.90	24.1	11.27
4	0.9	7	27.5	44.51	31.47	24.1	10.73
4	0.8	5	21.9	49.13	39.59	24.1	11.84
4	0.8	6	24.9	46.74	34.85	24.1	11.26
4	0.8	7	27.4	44.42	31.32	24.1	10.71
4	0.7	5	21.9	49.03	39.47	24.1	11.82
4	0.7	6	24.8	46.60	34.69	24.1	11.23
4	0.7	7	27.2	44.20	31.05	24.1	10.65
4	0.6	5	21.8	48.76	37.68	24.1	11.75
4	0.6	6	24.7	46.51	34.57	24.1	11.21
4	0.6	7	27.2	44.21	31.05	24.1	10.65
4	0.5	5	21.8	48.88	39.24	24.1	11.78
4	0.5	6	24.7	46.59	34.61	24.1	11.23
4	0.5	7	27.1	44.13	30.94	24.1	10.64

For K = 12, e = 0.6 and h = 15 and Sic as porous material.

Porous media	$\dot{Q}_{Rad}$	η_{Rad}	η_{II}	η_{Q}	η_{total}
Sic	22.4	50.27	40.98	24.1	12.11
AL2O3	44.5	50.92	**41.93**	24.1	12.27
SI3N4	44.6	50.69	41.59	24.1	12.22
SS304	**44.7**	**50.95**	**41.93**	24.1	**12.28**

For **L** = 6 **mm**, Porosity = 0.5, **V** = 5 **m/s**, **e** = 0.6, **h** = 15.

References

[1] L.C. Chia, B. Feng, The development of a micropower (micro-thermophotovoltaic) device, J. Power Sources 165 (2007) 455–480, https://doi.org/10.1016/j.jpowsour.2006.12.006.

[2] J. van der Heide, Thermophotovoltaics, Compr. Renew. Energy. 1 (2012) 603–618, https://doi.org/10.1016/B978-0-08-087872-0.00133-5.

[3] W.H. Kim, T.S. Park, Flame characteristics depending on recirculating flows in a non-premixed micro combustor with varying baffles, Appl. Therm. Eng. 148 (2019) 591–608, https://doi.org/10.1016/j.applthermaleng.2018.11.075.

[4] S.K. Chou, W.M. Yang, K.J. Chua, J. Li, K.L. Zhang, Development of micro power generators - A review, Appl. Energy 88 (2011) 1–16, https://doi.org/10.1016/j.apenergy.2010.07.010.

[5] B. Bitnar, W. Durisch, R. Holzner, Thermophotovoltaics on the move to applications, Appl. Energy 105 (2013) 430–438, https://doi.org/10.1016/j.apenergy.2012.12.067.

[6] E. Nadimi, S. Jafarmadar, Thermal and exergy assessmeot of a micro combustor fueled by premixed hydrogen/air under different sizes: A numerical simulation, J. Appl. Fluid Mech. 13 (2020) 1233–1243, https://doi.org/10.36884/JAFM.13.04.31067.

[7] K.F. Mustafa, M.Z. Abdullah, M.Z.A. Bakar, M.K. Abdullah, Performance, combustion characteristics and economics analysis of a combined thermoelectric and thermophotovoltaic power system, Appl. Therm. Eng. 193 (2021), 117051, https://doi.org/10.1016/j.applthermaleng.2021.117051.

[8] Y. Zhang, J. Pan, Y. Zhu, S. Bani, Q. Lu, J. Zhu, H. Ren, The effect of embedded high thermal conductivity material on combustion performance of catalytic micro combustor, Energy Convers. Manag. 174 (2018) 730–738, https://doi.org/10.1016/j.enconman.2018.08.085.

[9] W. Zuo, E. Jiaqiang, Q. Peng, X. Zhao, Z. Zhang, Numerical investigations on a comparison between counterflow and coflow double-channel micro combustors for micro-thermophotovoltaic system, Energy 122 (2017) 408–419, https://doi.org/10.1016/j.energy.2017.01.079.

[10] Z. He, Y. Yan, X. Li, K. Shen, J. Li, Z. Zhang, Comparative investigation of combustion and thermal characteristics of a conventional micro combustor and micro combustor with internal straight/spiral fins for thermophotovoltaic system, Int. J. Hydrogen Energy 46 (2021) 22165–22179, https://doi.org/10.1016/j.ijhydene.2021.04.030.

[11] P. Qian, M. Liu, X. Li, F. Xie, Z. Huang, C. Luo, X. Zhu, Effects of bluff-body on the thermal performance of micro thermophotovoltaic system based on porous media combustion, Appl. Therm. Eng. 174 (2020), 115281, https://doi.org/10.1016/j.applthermaleng.2020.115281.

[12] A. Tang, J. Pan, W. Yang, Y. Xu, Z. Hou, Numerical study of premixed hydrogen/air combustion in a micro planar combustor with parallel separating plates, Int. J. Hydrogen Energy 40 (2015) 2396–2403, https://doi.org/10.1016/j.ijhydene.2014.12.018.

[13] W. Zuo, E. Jiaqiang, Q. Peng, X. Zhao, Z. Zhang, Numerical investigations on thermal performance of a micro-cylindrical combustor with gradually reduced wall thickness, Appl. Therm. Eng. 113 (2017) 1011–1020, https://doi.org/10.1016/j.applthermaleng.2016.11.074.

[14] Q. Peng, W. Yang, E. Jiaqiang, Z. Li, H. Xu, G. Fu, S. Li, Investigation on H2/air combustion with C3H8 addition in the combustor with part/full porous medium, Energy Convers. Manag. 228 (2021), 113652, https://doi.org/10.1016/j.enconman.2020.113652.

[15] Q. Peng, W. Yang, E. Jiaqiang, H. Xu, Z. Li, K. Tay, G. Zeng, W. Yu, Investigation on premixed H2/C3H8/air combustion in porous medium combustor for the micro thermophotovoltaic application, Appl. Energy 260 (2020), 114352, https://doi.org/10.1016/j.apenergy.2019.114352.

[16] A. Tang, J. Deng, Y. Xu, J. Pan, T. Cai, Experimental and numerical study of premixed propane/air combustion in the micro-planar combustor with a cross-plate insert, Appl. Therm. Eng. 136 (2018) 177–184, https://doi.org/10.1016/j.applthermaleng.2018.03.001.

[17] J. Chen, W. Song, D. Xu, Thermal management in catalytic heat-recirculating micro-combustors: A computational fluid dynamics study, Appl. Therm. Eng. 160 (2019), 114073, https://doi.org/10.1016/j.applthermaleng.2019.114073.

[18] L. Ma, H. Xu, X. Wang, Q. Fang, C. Zhang, G. Chen, A novel flame-anchorage micro-combustor: Effects of flame holder shape and height on premixed CH4/air flame blow-off limit, Appl. Therm. Eng. 158 (2019), 113836, https://doi.org/10.1016/j.applthermaleng.2019.113836.

[19] T. Cai, A. Tang, D. Zhao, C. Zhou, Q. Huang, Experimental observation and numerical study on flame structures, blowout limit and radiant efficiency of premixed methane/air in micro-scale planar combustors, Appl. Therm. Eng. 158 (2019), 113810, https://doi.org/10.1016/j.applthermaleng.2019.113810.

[20] A. Tang, Y. Xu, C. Shan, J. Pan, Y. Liu, A comparative study on combustion characteristics of methane, propane and hydrogen fuels in a micro-combustor, Int. J. Hydrogen Energy 40 (2015) 16587–16596, https://doi.org/10.1016/j.ijhydene.2015.09.101.

[21] L. Han, J. Li, D. Zhao, Y. Xi, X. Gu, N. Wang, Effect analysis on energy conversion enhancement and NOx emission reduction of ammonia/hydrogen fuelled wavy micro-combustor for micro-thermophotovoltaic application, Fuel 289 (2021), 119755, https://doi.org/10.1016/j.fuel.2020.119755.

[22] L. Han, J. Li, D. Zhao, T. Cai, N. Wang, Energy and exergy conversion enhancement of a premixed hydrogen-fuelled wavy-combustor for micro-thermophotovolatic application, Appl. Therm. Eng. 196 (2021), 117328, https://doi.org/10.1016/j.applthermaleng.2021.117328.

[23] S. Akhtar, J.C. Kurnia, T. Shamim, A three-dimensional computational model of H_2-air premixed combustion in non-circular micro-channels for a thermo-photovoltaic (TPV) application, Appl. Energy 152 (2015) 47–57, https://doi.org/10.1016/j.apenergy.2015.04.068.

[24] S. Akhtar, M.N. Khan, J.C. Kurnia, T. Shamim, Investigation of energy conversion and flame stability in a curved micro-combustor for thermo-photovoltaic (TPV) applications, Appl. Energy 192 (2017) 134–145, https://doi.org/10.1016/j.apenergy.2017.01.097.

[25] Z. Mansouri, Combustion in wavy micro-channels for thermo-photovoltaic applications – Part I: Effects of wavy wall geometry, wall temperature profile and reaction mechanism, Energy Convers. Manag. 198 (2019), 111155, https://doi.org/10.1016/j.enconman.2018.12.105.

[26] Y. Su, J. Song, J. Chai, Q. Cheng, Z. Luo, C. Lou, P. Fu, Numerical investigation of a novel micro combustor with double-cavity for micro-thermophotovoltaic system, Energy Convers. Manag. 106 (2015) 173–180, https://doi.org/10.1016/j.enconman.2015.09.043.

[27] Z. He, Y. Yan, T. Zhao, S. Feng, X. Li, L. Zhang, Z. Zhang, Heat transfer enhancement and exergy efficiency improvement of a micro combustor with internal spiral fins for thermophotovoltaic systems, Appl. Therm. Eng. 189 (2021), 116723, https://doi.org/10.1016/j.applthermaleng.2021.116723.

[28] X. Yang, L. Zhao, Z. He, S. Dong, H. Tan, Comparative study of combustion and thermal performance in a swirling micro combustor under premixed and non-

premixed modes, Appl. Therm. Eng. 160 (2019), 114110, https://doi.org/10.1016/j.applthermaleng.2019.114110.
[29] S. Wu, S. Abubakar, Y. Li, Thermal performance improvement of premixed hydrogen/air fueled cylindrical micro-combustor using a preheater-conductor plate, Int. J. Hydrogen Energy 46 (2021) 4496–4506, https://doi.org/10.1016/j.ijhydene.2020.10.237.
[30] S. Mohseni, E. Nadimi, S. Jafarmadar, R.A. Rezaei, Enhance the energy and exergy performance of hydrogen combustion by improving the micro-combustor outlet in thermofluidic systems, Int. J. Hydrogen Energy 46 (2021) 6915–6927, https://doi.org/10.1016/j.ijhydene.2020.11.114.
[31] Q. Peng, B. Xie, W. Yang, S. Tang, Z. Li, P. Zhou, N. Luo, Effects of porosity and multilayers of porous medium on the hydrogen-fueled combustion and micro-thermophotovoltaic, Renew. Energy 174 (2021) 391–402, https://doi.org/10.1016/j.renene.2021.04.108.
[32] Q. Peng, W. Yang, E. Jiaqiang, H. Xu, Z. Li, W. Yu, Y. Tu, Y. Wu, Experimental investigation on premixed hydrogen/air combustion in varied size combustors inserted with porous medium for thermophotovoltaic system applications, Energy Convers. Manag. 200 (2019), 112086, https://doi.org/10.1016/j.enconman.2019.112086.
[33] S.K. Chou, W.M. Yang, J. Li, Z.W. Li, Porous media combustion for micro thermophotovoltaic system applications, Appl. Energy 87 (2010) 2862–2867, https://doi.org/10.1016/j.apenergy.2009.06.039.
[34] J.F. Pan, D. Wu, Y.X. Liu, H.F. Zhang, A.K. Tang, H. Xue, Hydrogen/oxygen premixed combustion characteristics in micro porous media combustor, Appl. Energy 160 (2015) 802–807, https://doi.org/10.1016/j.apenergy.2014.12.049.
[35] K.F. Mustafa, S. Abdullah, M.Z. Abdullah, K. Sopian, Experimental analysis of a porous burner operating on kerosene-vegetable cooking oil blends for thermophotovoltaic power generation, Energy Convers. Manag. 96 (2015) 544–560, https://doi.org/10.1016/j.enconman.2015.03.022.
[36] S. Bani, J. Pan, A. Tang, Q. Lu, Y. Zhang, Numerical investigation of key parameters of the porous media combustion based Micro-Thermophotovoltaic system, Energy 157 (2018) 969–978, https://doi.org/10.1016/j.energy.2018.05.151.
[37] W. Wang, Z. Zuo, J. Liu, Numerical study of the premixed propane/air flame characteristics in a partially filled micro porous combustor, Energy 167 (2019) 902–911, https://doi.org/10.1016/j.energy.2018.11.006.
[38] P. Gentillon, J. Southcott, Q.N. Chan, R.A. Taylor, Stable flame limits for optimal radiant performance of porous media reactors for thermophotovoltaic applications using packed beds of alumina, Appl. Energy 229 (2018) 736–744, https://doi.org/10.1016/j.apenergy.2018.08.048.
[39] V. Bubnovich, M. Toledo, L. Henríquez, C. Rosas, J. Romero, Flame stabilization between two beds of alumina balls in a porous burner, Appl. Therm. Eng. 30 (2010) 92–95, https://doi.org/10.1016/j.applthermaleng.2009.04.001.
[40] W.M. Yang, S.K. Chou, K.J. Chua, J. Li, X. Zhao, Research on modular micro combustor-radiator with and without porous media, Chem. Eng. J. 168 (2011) 799–802, https://doi.org/10.1016/j.cej.2010.12.083.
[41] J. Li, Q. Li, Y. Wang, Z. Guo, X. Liu, Fundamental flame characteristics of premixed H_2-air combustion in a planar porous micro-combustor, Chem. Eng. J. 283 (2016) 1187–1196, https://doi.org/10.1016/j.cej.2015.08.056.
[42] Q. Peng, E. Jiaqiang, J. Chen, W. Zuo, X. Zhao, Z. Zhang, Investigation on the effects of wall thickness and porous media on the thermal performance of a non-premixed hydrogen fueled cylindrical micro combustor, Energy Convers. Manag. 155 (2018) 276–286, https://doi.org/10.1016/j.enconman.2017.10.095.
[43] J. Li, S.K. Chou, W.M. Yang, Z.W. Li, A numerical study on premixed micro-combustion of CH 4 – air mixture: Effects of combustor size, geometry and boundary conditions on flame temperature, Chem. Eng. J. 150 (2009) 213–222, https://doi.org/10.1016/j.cej.2009.02.015.
[44] E. Jiaqiang, W. Zuo, X. Liu, Q. Peng, Y. Deng, H. Zhu, Effects of inlet pressure on wall temperature and exergy efficiency of the micro-cylindrical combustor with a step, Appl. Energy 175 (2016) 337–345, https://doi.org/10.1016/j.apenergy.2016.05.039.
[45] A. Alipoor, M.H. Saidi, Numerical study of hydrogen-air combustion characteristics in a novel micro-thermophotovoltaic power generator, Appl. Energy 199 (2017) 382–399, https://doi.org/10.1016/j.apenergy.2017.05.027.
[46] H. Xue, W. Yang, S.K. Chou, C. Shu, Z. Li, Microthermophotovoltaics power system for portable MEMS devices, Microscale Thermophys. Eng. 9 (2005) 85–97, https://doi.org/10.1080/10893950590913431.
[47] O. Cam, H. Yilmaz, S. Tangoz, I. Yilmaz, ScienceDirect A numerical study on combustion and emission characteristics of premixed hydrogen air flames, Int. J. Hydrogen Energy (2017) 1–11, https://doi.org/10.1016/j.ijhydene.2017.07.017.
[48] E. Nadimi, S. Jafarmadar, The numerical study of the energy and exergy efficiencies of the micro-combustor by the internal micro-fin for thermophotovoltaic systems, J. Clean. Prod. 235 (2019) 394–403, https://doi.org/10.1016/j.jclepro.2019.06.303.
[49] A. Fan, H. Zhang, J. Wan, Numerical investigation on flame blow-off limit of a novel microscale Swiss-roll combustor with a bluff-body, Energy 123 (2017) 252–259, https://doi.org/10.1016/j.energy.2017.02.003.
[50] W.M. Yang, S.K. Chou, C. Shu, H. Xue, Z.W. Li, D.T. Li, J.F. Pan, Microscale combustion research for application to micro thermophotovoltaic systems, Energy Convers. Manag. 44 (2003) 2625–2634, https://doi.org/10.1016/S0196-8904(03)00024-4.
[51] H. Yilmaz, O. Cam, S. Tangoz, I. Yilmaz, Effect of different turbulence models on combustion and emission characteristics of hydrogen/air flames, Int. J. Hydrogen Energy 42 (2017) 25744–25755, https://doi.org/10.1016/j.ijhydene.2017.04.080.